Politecnico di Torino
Scuola di Ingegneria
Corso di Laurea in Ingegneria Biomeccanica
Anno Accademico 2017/2018

MASTER THESIS REPORT

Development of a numerical kinetic and kinematic simulator for analyzing TKA performance

Relators:

Prof. Alberto Audenino
Prof.ssa Cristina Bignardi

Student:

Edoardo Bori

Supervisor:

Prof. Bernardo Innocenti

Index

1. Introduction - Native and Replaced Human Knee Joint

Kinematic of knee joint is one of the most complex to analyse due to its internal interaction, regulating the movement through contact forces between bones, muscles and connective tissue[60].

Nonetheless, its study is fundamental to allow a better comprehension of the forces acting during various tasks and then to meet the needs of the ever-increasing diffusion of the Total Knee Arthroplasty (TKA).

1.1 Physiological Joint Anatomy

1.1.1 Bones and Cartilage

The bones composing the joint are Femur, Patella, Tibia and Fibula [see Figure 1][64]. The femoral bone distal epiphysis ends with two condyles, different from each other as the medial one is elliptically shaped and with a large posterior offset[65] while the lateral one has a more spherical shape[66] and a smaller posterior offset [see Figure 2]. Those two bony structures interact with the tibial surfaces involved in the tibiofemoral articulation, which consist in two plateaus separated by an intercondylar eminence[64]: in medio-lateral direction, both these plateaus are concave while in antero-posterior there is a difference between them, being the lateral tibial plateau convex opposingly to the medial one, and this asymmetry leads to an increased lateral mobility [see Figure 3]. Moreover, the medial plateau has greater surface and disposes of a thicker articular surface than the lateral [see Figure 4].

The patellar bone is a triangular shaped bone situated on the anterior side of the joint and mostly interact with the two femoral condyles, sliding in what is called the Patellar (or trochlear) groove [see Figure 1 – 6][67]. Its posterior surface is composed by many facets, mostly covered by a layer of cartilage to decrease the friction during the movements [see Figure 5].

A layer of cartilage is also present on all the articular surfaces to guarantee the sliding and lubrication and moreover to provide shock absorption. Two menisci [see Figure 6] are located between each condyle and the underlying tibial plateaux to guarantee the restoration of congruence between the bones extremities and to provide damping effects[70].

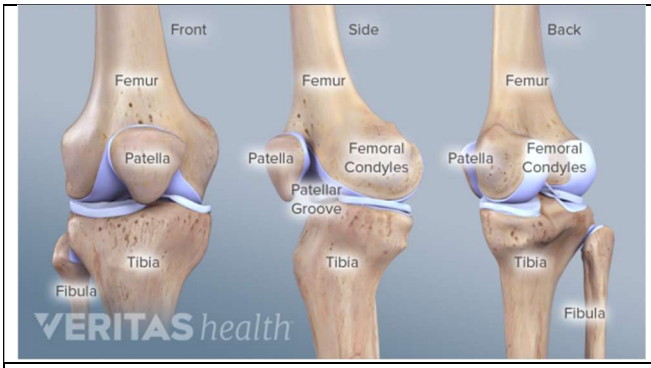

Figure 1.1 – Knee Joint Bony Components

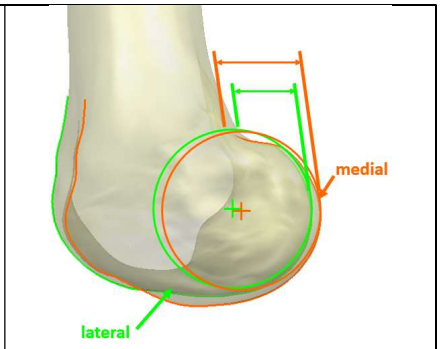

Figure 1.2 – Femoral Condyles

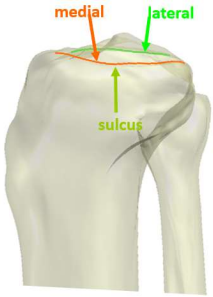

Figure 1.3 – Tibial Plateau, medial view

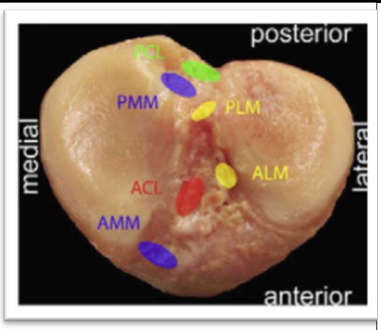

Figure 1.4 – Tibial Plateau, top view

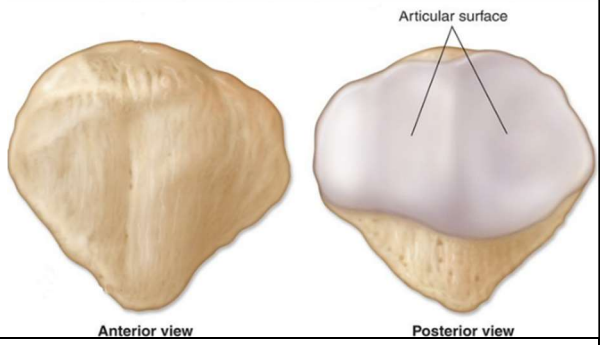

Figure 1.5 – Patellar Bone and articular surface cartilage

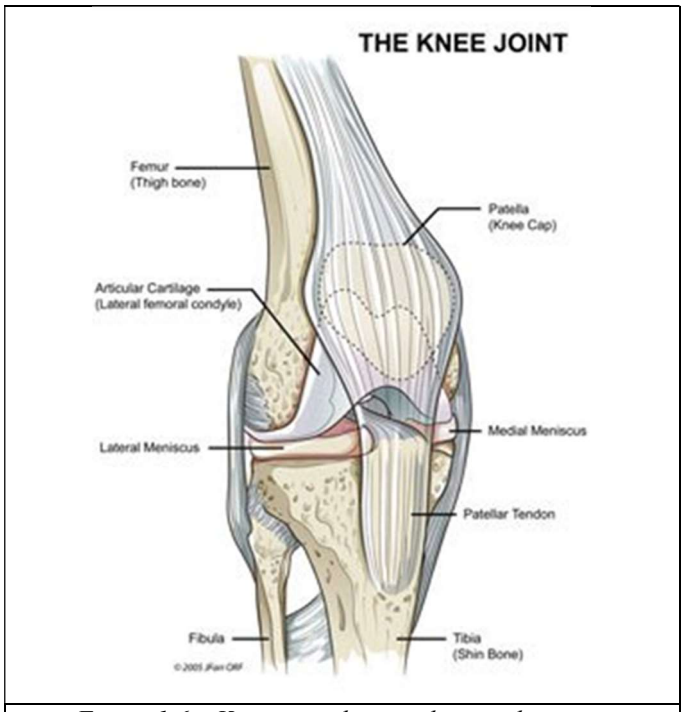

Figure 1.6 – Knee articular cartilage and menisci

1.1.2 Ligaments

The ligaments involved in this joint are the cruciate and the collateral ones connecting tibia and femur [see Figure 7], while the patella-related ones are the patellar tendon, the medial patellofemoral ligament (MPFL) and the lateral retinaculum [see Figure 8][67].

The presence of these elements, consisting in connective tissue and comparable to bundles of fibres, allows to keep together different bony segments and to control their relative position and alignment during movements, as detailed below.

The collateral ligaments are located on both medial and lateral sides of the joint [see Figure 7] and are mainly given the role of stabilizers along the mid-lateral axis.

Cruciate ligaments are instead responsible for the anteroposterior stabilization, with the anterior ligament preventing excessive frontal displacement of the tibia relative to the femur and the posterior one acting on the opposite direction.

Patellar tendon is the link between patellar bone and tibial tubercle [see Figure 8], and it is the continuation of the quadriceps tendon (hence the tendon nomenclature despite it's actually connecting two bones).

Thanks to its peculiar shape, it's able to exert contact forces with the bones of the articulation allowing the correct positioning of the patellar bone in the patellar groove during the flexion-extension movements[67].

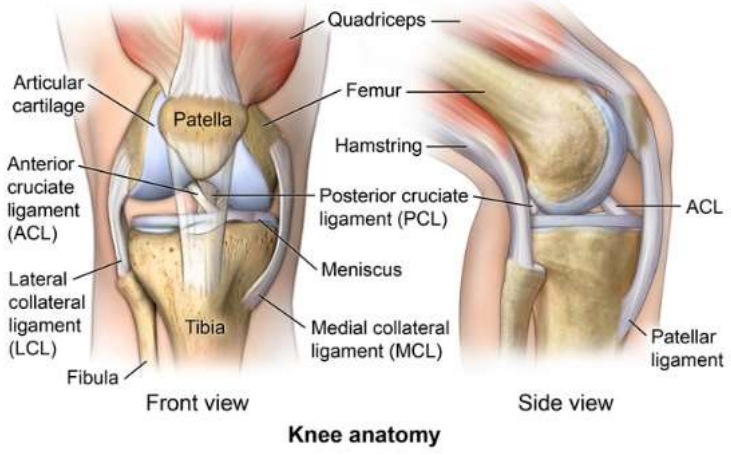

Figure 1.7 – Knee anatomy

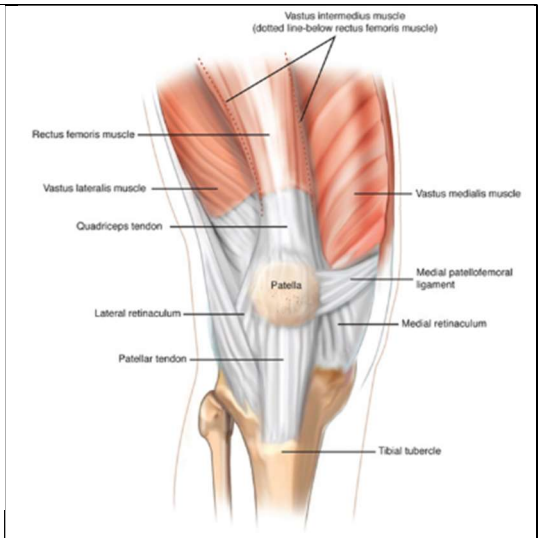

Figure 1.8 – Focus on patellar ligaments

1.1.3 Muscles

Femoral quadriceps [see Figure 9] include the main four extensor muscles of the knee articulation and have an important role in walking, running, jumping and squatting. Moreover, they play the important role of stabilizing the patella and the knee joint during gait[67].

Hamstrings [see Figure 10] are a group of muscles located in the back of the thigh, with the main function of flexing the leg on the thigh and extending the thigh on the hip; they are the antagonist muscles to the quadriceps during walking in the deceleration of knee extension[67].

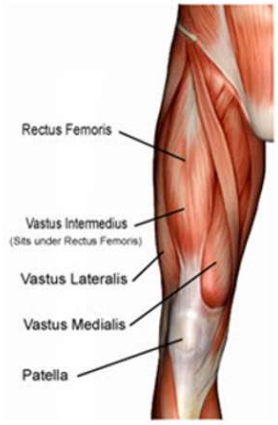

Figure 1.9 – Quadriceps Muscles

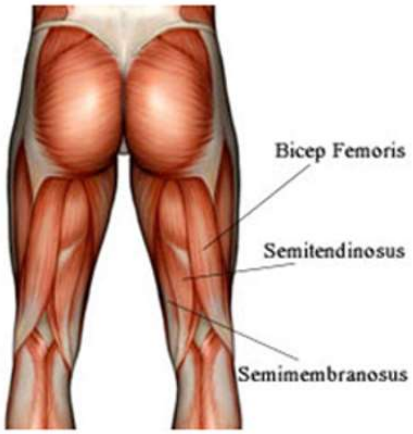

Figure 1.10 – Hamstring muscles

1.1.4 The Joint

The knee can thus be considered as composed by two different joints, namely the patellofemoral joint and the tibiofemoral joint[68]; the latter can then be in turn be subdivided in medial and lateral to analyse in a more detailed way interactions between each femoral condyle and the respective portion of the underlying tibial plateau.

1.2 Knee injuries and diseases

In pathological cases or in articulations affected by the natural degradation of protective tissues, joint cartilage can wear out or get sore and then stiffen, losing its properties and leading to difficulties in movement and pain for the patient. There are several risk factors (such as obesity, previous knee injuries, removal of a meniscus…)[1] that could accelerate the loss of stability and the other structural and functional problems linked to this degradation, but the main clinical reason leading to the necessity of an intervention is nonetheless usually osteoarthritis[2].

It is therefore a degenerative process over time that leads to the disappearance of the cartilaginous interface which, not being innervated, guaranteed prevention from pain; the fact of not being vascularized either, together with the poor mitogenicity of chondrocytes, nullifies though its regenerative potential and makes then this process irreversible if not properly treated[3].

Consequently, the joint interfaces start to involve bony surfaces which are instead rich in blood vessels and nerves and therefore predisposed to generate painful sensations in case of contact or rubbing; these problems may then lead to latter ones as a patient suffering from chronic pain in a leg will tend to make less and less use of it, leading to atrophy of its muscles and to overload the other leg (thus accelerating its process of cartilage degradation).

Knee pain is a problem that affects a large portion of the adult and elderly population[3,4,5], and tends to have a major impact on the quality of life[6] thus making necessary finding means to prevent the occurrence of this condition, to curb its effects[7] or, when there is no other possibility, to surgically operate to restore the functionality of the joint and the well-being of the individual.

1.3 Total Knee Arthroplasty

Total knee arthroplasty (TKA) is an orthopedic surgical procedure involving the replacement of the articular surfaces of the knee[58], consisting in the femoral condyles and the tibial plateau, with a prosthetic device named total knee replacement (TKR)[8]. A polyethylene insert, placed between the tibia and the femur, performs the role of the damper to absorb shocks and allows slipping [see Figure 11]; in extremely damaged joints, also the patella can be replaced with a polyethylene component to restore the extensor mechanism.

The prosthetic implant is usually chosen whenever other surgical techniques have failed or simply are not applicable, as the insertion of a foreign body into the organism involves a series of complications concerning the biocompatibility and wear of these bodies, especially if implanted in young and/or physically active patients[71].

Many typologies of TKR are available on the market, each one with its own characteristics and specifications, and consequently the selection criterion is a crucial point: the kind of prothesis implanted depends on the joint situation and the gravity of bone loss[9] but usually other influences have to be taken in consideration, such as economic issues[10] and most of all the surgeon's preference as previous experiences and positive outcomes can lead him to prefer one model overall and then bias the choice[11].

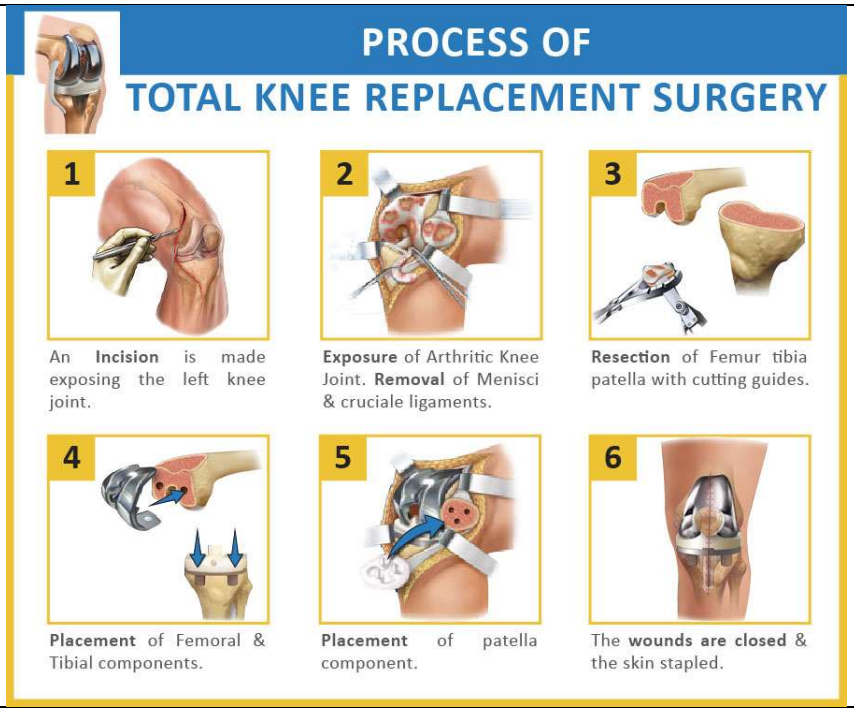

Figure 1.11 – TKR surgery

1.3.1 Success and Failure

Since the main aim of the operation is the restoration of the mobility and the well-being of the patient, the study of the follow-up of the implant is fundamental to establish its success or failure; in fact, symptom of this latter is often patient's dissatisfaction than can forecast the incoming breaking or detachment of the prosthesis itself (be this due to polyethylene wear, infection or loosening, which are the main causes of failure[12]) but it can also be considered a case of failure itself: if the quality of life is not improved, the operation has not reached its intent, and therefore it is important to understand the reasons for these outcomes to avoid incurring in them again[13,14].

Several studies have been conducted on this topic resulting in a common agreement that the success of a TKA is strongly linked to the prothesis design, but the latter is optimized for a specific musculoskeletal condition as intended by its producer: the aim of the surgical operation is then to recreate (via cuts and other procedures) the specifics of this ideal situation, and any divergence from that standard is to be intended as a malpositioning.

In some prosthesis, a malrotation of the tibial component can change massively the stress on the tibial insert in relation to the one resulting from a proper positioning, and this heavily affects the degeneration of the polyethylene leading to its failure[16,17,18]; other designs instead allow a bigger margin of manoeuvre, with only minimal variations ascribable to the surgeon performance[19,62,63].

A way to forecast the theoretical results of an imperfect implant for the prosthesis on the market could be impactful on the decision process on which one to adopt for the given patient.

1.3.2 Economic Profile

The global knee implants market in 2015 accounted for USD 8.8 billion and is growing every year, thanks to factors as the improvement of minimally invasive surgeries, the rising prevalence of arthritis and the increase of the geriatric population; however, the strict system of regulations concerning medical devices approval and the different cases of failures or defected products are probably going to interfere with this growth.[20]

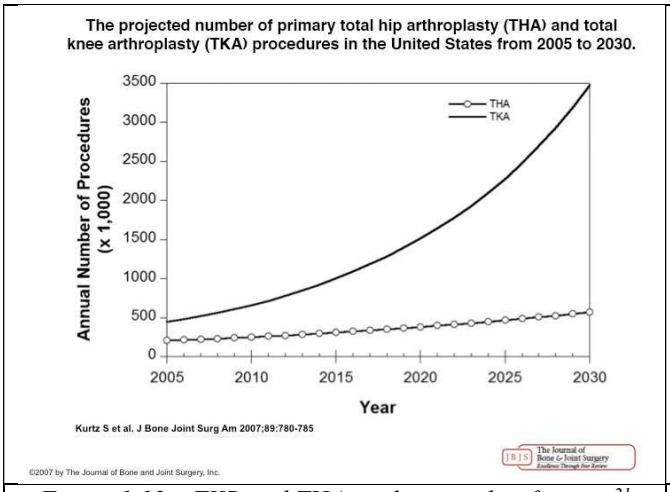

Figure 1.12 – TKR and THA implant number forecast[21]

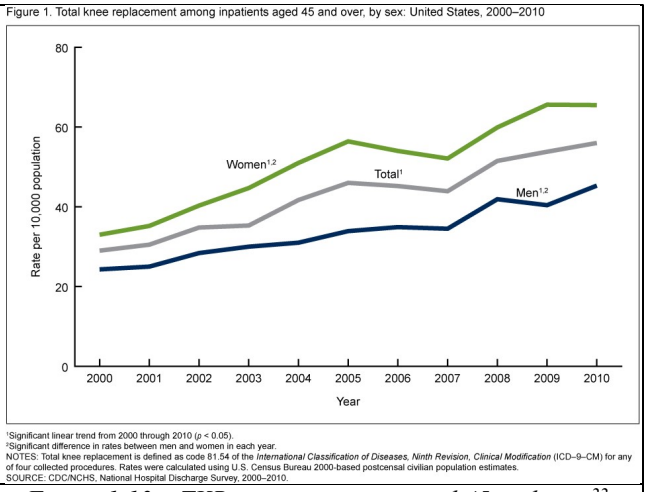

Figure 1.13 – TKR among patients aged 45 and over[22]

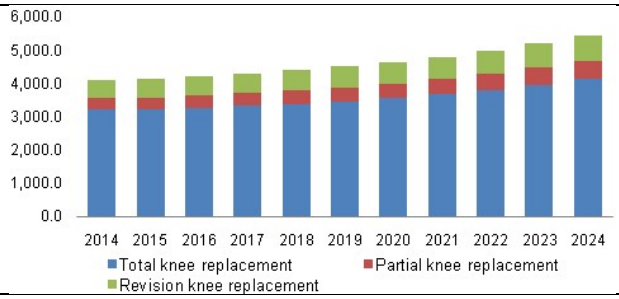

Figure 1.14 - U.S. knee implants market revenue, by procedure type, 2014 - 2024 (USD Million)[20]

This economic relevance is therefore an excellent spur to deepen the studies on this topic and the improvement of analysis tools is an important step to reach results.

2. Literature Research and State of the Art

2.1 Knee Biomechanics

Usually, in articular joints, mobility and stability tend to go one at expense of the other; nevertheless, in the knee joint both of these properties are maintained thanks to a series of interactions between soft and bony tissues; this joint is one of the most complex in the human body, with its 6 degrees of freedom allowing three rotations and three translations along the axes, and can be subdivided in three main compartments: patellofemoral, medial tibial-femoral and lateral tibial-femoral[68].

The study of its kinematics is fundamental to fully understand how to solve problems linked to the pathological joint and how to properly replicate the action of a healthy one via prosthesis.

2.1.1 Joint Coordinate System: Grood and Suntay

To deal with the kinematics of the articulation, however, it is necessary to firstly address the topic of which system of reference to adopt for the analysis: in this regard, the studies conducted by Grood and Suntay[23] provide a suitable solution allowing a simpler and complete way to express the relative movements taking place in the knee joint.

Firstly, two different cartesian coordinate systems are defined (XYZ for femur and xyz for tibia) [see Figure 15]; a floating axis F is then implemented to be perpendicular to femoral condylar axis (X) and lying on tibial plane xy [see Figure 16].

In this way, flexion-extension can be measured about the femoral body fixed axis X, intra-extra rotation about the tibial fixed one z and ab-adduction on the floating axis F.

Moreover, also translation between the two bones can be expressed on those three axes analysing the position of femoral coordinate centre referred to tibial one.

Joint coordinate system can then be modelled as a four-link kinematic chain composed by cylindrical joints, and this representation will be fundamental to implement this system of reference in a virtual environment [see Figure 17].

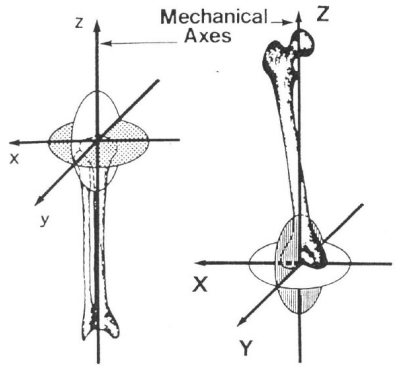

Figure 2.1 – XYZ and xyz Cartesian Coordinate Systems

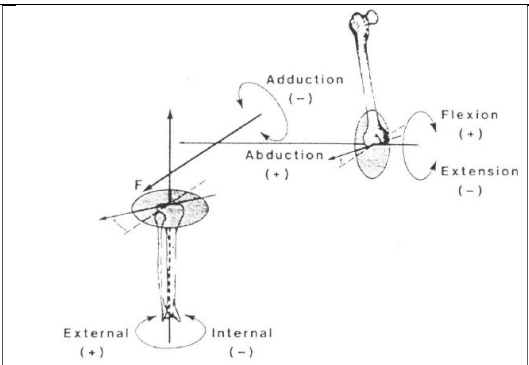

Figure 2.2 – Implemented F Axis

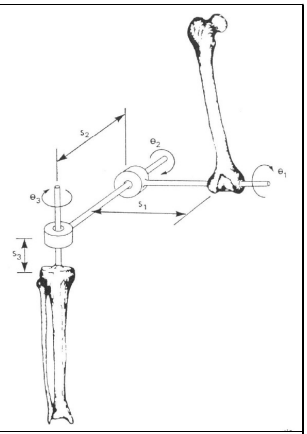

Figure 2.3 – The Four Link Kinematic Chain

2.1.2 Movements

The main movements are the flexion-extension around the medio-lateral axis (from -15° to 140°) and the intra-extra rotation around the longitudinal one (25°-30°); also a varus/valgus rotation is possible (between -6° and 8°)[24] [see Figure 19].

Flexion-extension is based on the contribution of rolling and slipping between femur and tibia, and the relative movement between bones changes during the different phases of the flexion: starting from the extended position, rolling is the main movement but when the angle of flexion increases slipping become predominant and it's the only one in the final phase of the flexion [see Figure 18].

The rolling phase is then different between the medial condyle (where it goes on up to 10°-15°) and lateral condyle (up to 20°), but nontheless it leaves place to slipping phase in the end[69].

The intra-extra rotation is possible only when the joint is flexed because the full extended knee doesn't allow this movement, as it usually takes place also during the flexion-extension movement.

Translations are in the order of the millimetre, the antero-posterior one being the highest one (10 -15 mm) while the medio-lateral and the proximal-distal have a range from 2 to 4 or 5 mm [see Figure 19][24].

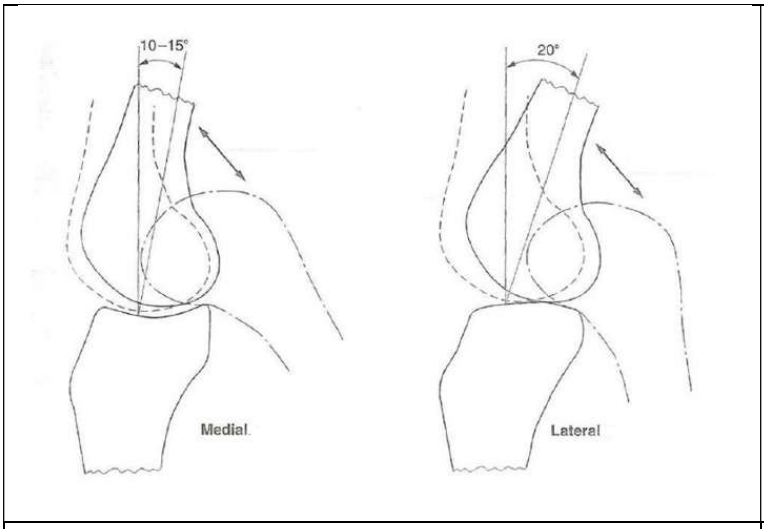

Figure 2.4 – Rolling and Slipping in Flexion

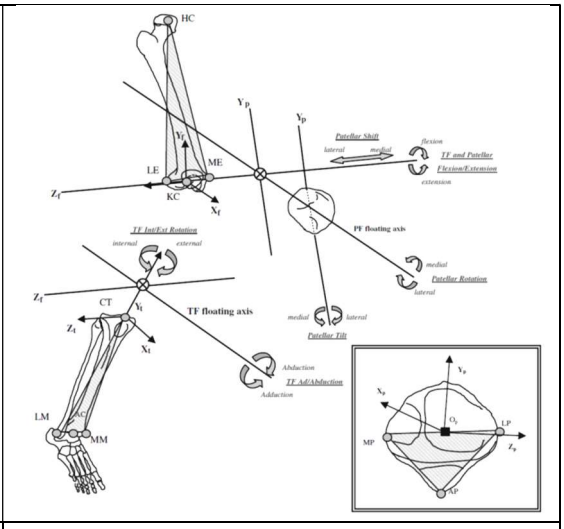

Figure 2.5 – Knee Movements

2.1.3 Articular Forces

The articular forces can be subdivided in tibiofemoral and patellofemoral and are typically analysed during various tasks as walking, climbing stairs and squats.

Usually during a physiological walk the tibial-femoral contact forces range from two to five times the body weight[25], while the patella-femoral ones turn out to be lower (around half of the body weight)[26].

Those forces are quite different if obtained during other movements, such as walking up and down stairs (patella-femoral forces reach respectively two and three times the body weight) or standing up from a chair without using the arms (patella-femoral forces go up to three times and a half the body weight)[26], and they reach their maximum of 20/24 times the body weight while running or jumping.

2.2 Data Obtaining

To date, three main methods are adopted to obtain data on this joint, each of them with its pros and cons: in vivo, in vitro and numerical analysis.

In vivo tests refer to the real joint, but can be influenced by artefacts during the measurements and be susceptible to geometric differences from subject to subject; in vitro tests instead guarantee greater control but in turn cannot reach the maximum realism as they are performed on cadaveric legs and therefore also require a large number of samples to be able to provide appreciable results; finally numerical analysis was introduced: to bypass the problems related to experimental tests (or at least minimize the number of samples needed), numerical simulators have been employed using finite element analysis to obtain information about the movement taken in consideration [see Figure 20]; nonetheless, to achieve good results this method often requires a massive computing time and it's often difficult to represent properly the complexity of the joint; an improvement in precision and efficiency therefore is still needed and different paths have been followed to achieve this goal.

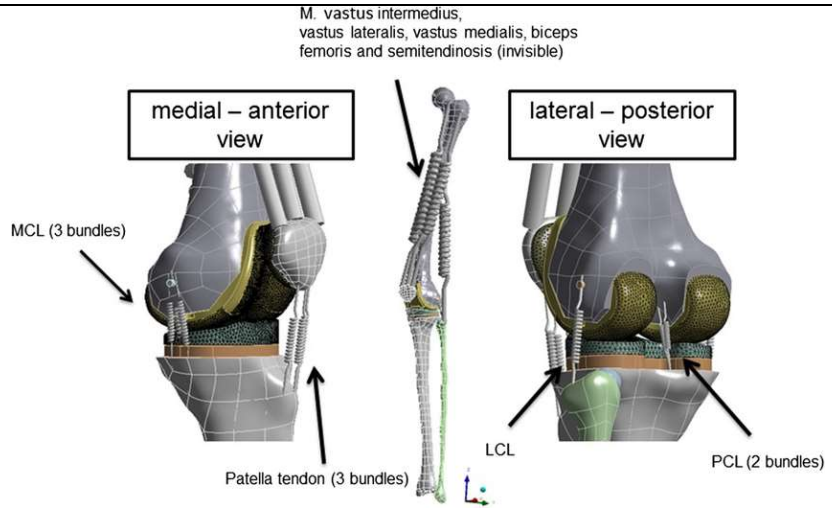

Figure 2.6 – Numerical Knee Joint Reproduction

2.2.1 In Vivo

This method guarantees a good relevance and realism and is usually performed via Motion analysis (with markers and cameras) [see Figure 21] or via direct imaging of bones and implants (Dynamic RSA, MRI, Fluoroscopy).

Force platforms [see Figure 21] and electromyography [see Figure 22] can be then used to acquire data about the forces and muscles activation.

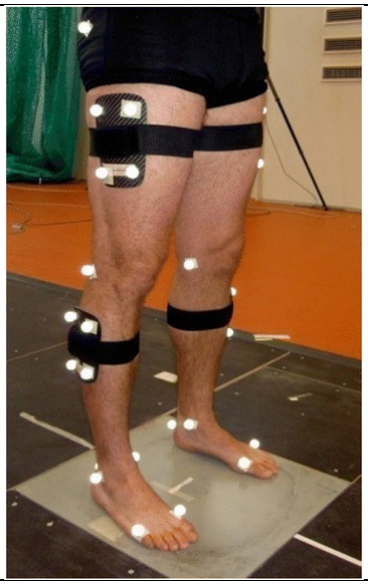

Figure 2.7 – Motion Capture Markers and force platform

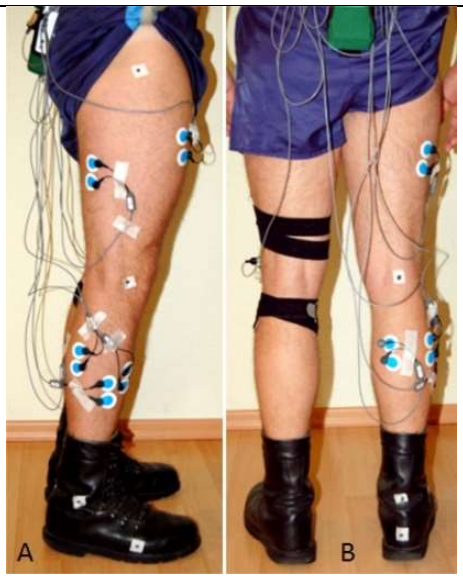

Figure 2.8 – Electromyography setup

2.2.2 In Vitro

This method involves the use of cadaver specimens and it is the mainly adopted for the transposition from real tests to numerical analysis.

In literature, many different devices have been developed and used to acquire data regarding motion and forces involved in the knee joint different movements.

2.2.2.1 The Oxford Rig

The Oxford rig [see Figure 23] main aim is to reach 6 d.o.f. thanks to ankle and hip joints: 3 sets of rotating bearings allow flexion-extension, abduction-adduction and intra-extra rotation in the ankle joint while on the hip side only 2 sets guarantee to freely perform abduction-adduction and flexion-extension, with the addition of a linear bearing to allow vertical displacement [27].

2.2.2.2 Kansas Knee Simulator

The Kansas Knee Simulator (KSS) [see Figure 24] is a servo-hydraulic machine used to perform dynamic loading activities tests on cadaveric legs or on prosthesis, modeled after the Purdue Knee Simulator Mark II[28]

It has five axes (for quadriceps, vertical load, medial-lateral, vertical torque and ankle flexion) allowing to operate them in force or displacement control as the input; the KKS doesn't control the knee kinematics, instead they are the output of the process and so they directly depend on the controls applied on the axis and on knee structure and geometry.

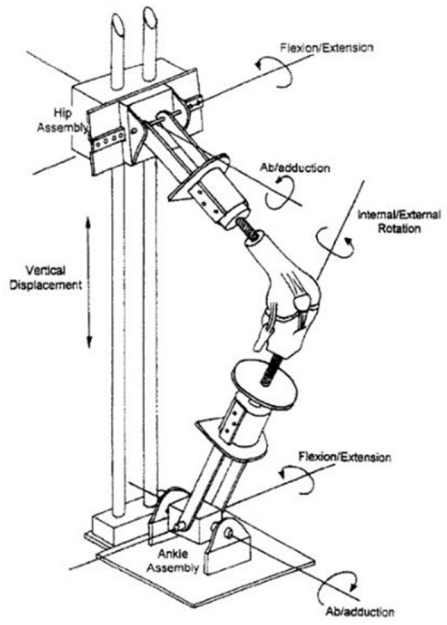

Figure 2.9 – The Oxford Rig

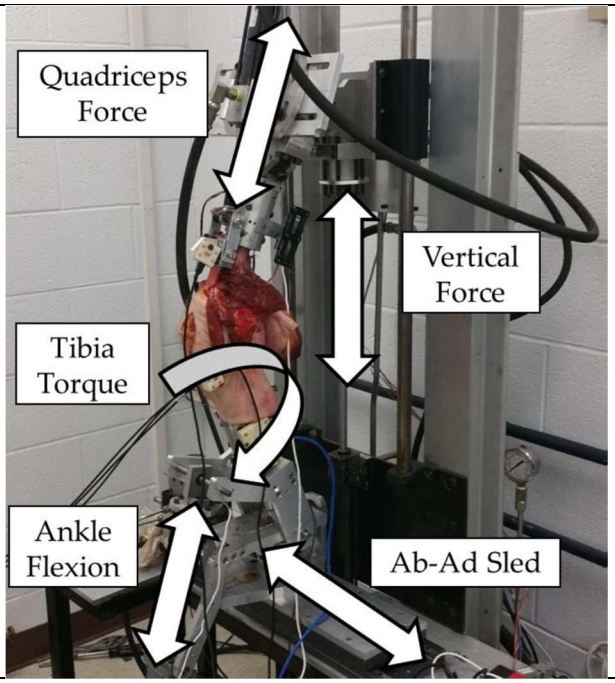

Figure 2.10 – The Kansas Knee Simulator

2.2.3 Numerical Analysis

Various models have been implemented to reproduce different in vitro testing devices[59] but in this study mainly Oxford Rigs and KKS are taken in consideration due to their versatility and performances.

2.2.3.1 KneeSim

One of the first software introduced on the market is the KneeSIM[29], a plug-in module to LifeMOD™[30].

It is a dynamic, 3D, physics-based software aimed to study the mechanics of the human knee by simulating the in-vivo performances of TKR systems [see Figure 25], becoming thus a great tool to improve quality and allow innovation keeping the product development process time and cost lower compared to completely analogic alternatives.

KneeSIM simulates a single leg attached to an Oxford rig, with accurate representation of the bones, muscles, ligaments and tendons so that the TKR system to be analyzed can be positioned and tested; different models can thus be analyzed, but also tests regarding mispositioning can be led on the same model: various design parameters, such as geometry, surgical placement or patient variables, ensure a high fidelity to the real system in every of its aspects.

This input given, simulations can be run in little time returning knee's motion and dynamics data as output then helping to understand the mechanics of the joint.

Developed for the medical device industry, LifeMOD/KneeSIM has been tested and validated in private laboratories using measurements obtained from a TKA system by fluoroscopy techniques, and thus it has been proven accurate for laxity tests, fluoroscopy comparisons, and more.

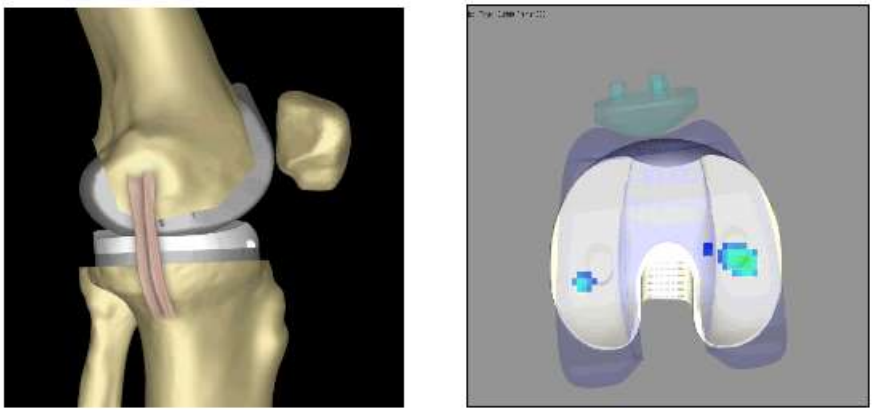

Figure 2.11 – KneeSIM output animation

2.2.3.2 Reeve et al., using MSC.ADAMS

Reeve's model aimed instead to the creation of a Computational Model of KKS which goal was to predict the required actuators inputs needed to produce a desired knee loading on the real machine[31].

The virtual model is comprehensive of all the mechanical components of the real machine (to properly simulate every inertial and dynamic effect of the different tests) and could be controlled via the actuators as if it was the real device; the validation has then been performed giving the same input to the real and the simulated actuators and comparing the relative outputs: the conclusion has been that it is possible, with the limitations of the case, to obtain satisfying results through this kind of simulation.

2.3 Future Developments

Up to date, in vivo and in vitro tests have been the most effective and reliable methods for data obtaining, but they are on the other hand expensive in terms of time and money: because of this, numerical simulation is growing as a very powerful tool in the hands of surgeons and engineers as it is able to decrease these costs giving nonetheless appreciable results, but further validation and optimisation studies are required to fully express its true potential.

The implementation of simulator able to allow personalisation on the model (bone geometries, prosthesis, positioning and mechanical properties) and to deliver realistic results without requiring prohibitive computing time could therefore be a good path to be taken to meet those needs.

3. Aim of the Work

The aim of this thesis is to model a prosthetic knee joint in order to obtain a realistic simulation of a squat movement, similar to the one obtained in an Oxford Knee Rig or in a Kansas Simulator; in this process it's important to remember the elastic properties of the different materials representing bones and prosthesis, though keeping in mind that computational time is also a variable intended to be kept at minimum value.

To reach this goal, different possibilities were available: up to day many Finite Element Analysis software are used to perform various kind of knee movements simulations, but for this project a Multi-body Simulation Software was chosen to keep a relatively low computing time while still being able to deliver significant results.

SimPack[32] is a general-purpose Multibody Simulation (MBS) software used for the dynamic analysis of mechanical and mechatronic systems, able to generate and solve virtual 3D models in order to predict and visualize motion, coupling forces and stresses; it also allows to use geometries previously obtained from imaging and modified via a CAD editor (Solidworks[33] and Abaqus[34] were used for this purpose) to generate the bodies involved in the simulation.

This software is therefore optimal for the intended use, since having the possibility to foresee the stress and displacement in a knee joint depending on the design of prosthesis used and the different positioning of the latter could be of great help during the prosthesis selection process and moreover could highlight the severity level of eventual malpositioning, while the fact of using patient specific bone geometries will improve the realism of the results making them more reliable.

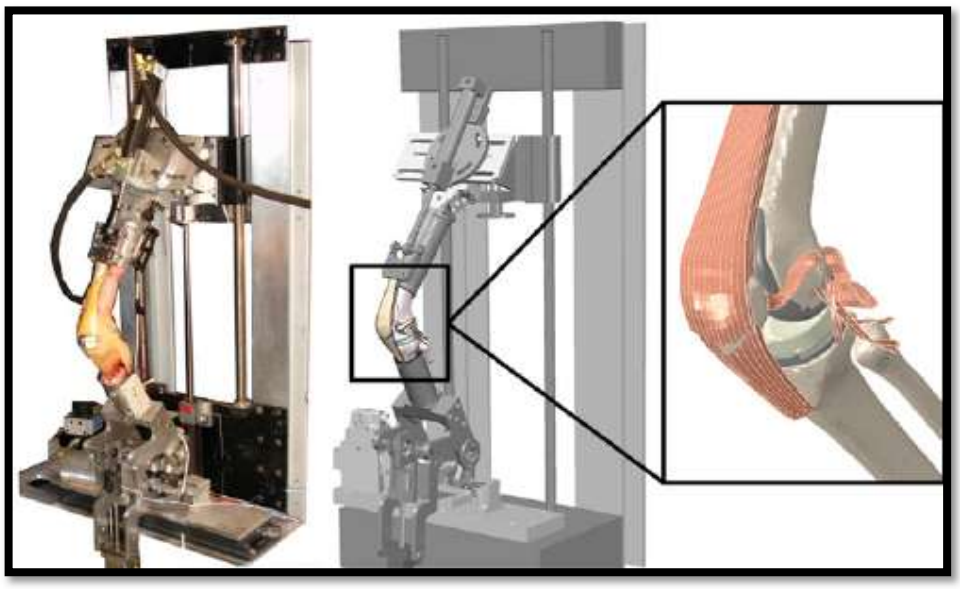

Figure 3.1 – Numerical Reproduction of an In vitro testing device

4. Models

Being the goal of the project the creation of a squat simulator, the first step is the implementation of a virtual equivalent of the device used for the real tests; contrariwise to Reeve et al.[31], the real machine components are not taken in consideration to avoid an excessive complexity of the model so only its purpose will be taken in account. A linear rail is then implemented, and a cart coupled with the latter will be attached to the femoral head in order to allow its movement via different sinusoidal routines; the distal extremity of the limb will be instead constrained to the rail to keep it on the same axis of the cart during the squat.

As well as the assembly within the software environment of bodies geometries and mechanical properties and the application of the relative forces, a required input will be the displacement function for the cart connected to the femoral head: the simulator will then be able to provide the animation and graphs of the movement as an output, together with data regarding the contact forces between the various elements during the whole time of action.

Using this layout as a standard for every model, elements will be iteratively added to the simulated leg attached to the device, in order to increase its fidelity to the real test and therefore increasing the relevance of the results.

The steps to refine the model, analyzed in more detail in this chapter, were the following:

- software features as bodies, forces and other relationships among simulation elements;

- 3D geometries editing, cuts and assemblies of bones and prosthesis via ligaments and constraints;

- implementation of the patellar component and primitive modeling of soft tissue;

- various means for regulating tendon and patella action;

- modeling of the patellar tendon as a set of bodies;

- implementation of additional ligaments.

4.1 First Model – Oversimplified

The best way to comprehend how to simulate a knee joint is to initially oversimplify it: for this reason, the first preparatory model is based on rigid bodies only and every constraint with the rail has been set up as two dimensional, namely it can rotate or translate only on a given plane.

4.1.1 Bodies and Geometries

Three different rigid bodies have been implemented in this first model to represent femur, tibia and patella. Geometries were then attributed to those latter: the long bones diaphysis structure is represented by simple geometries as cylinders, while epiphysis [see Figure 27 - 28] and patella [see Figure 29] required further modelling to obtain contact surface vaguely resembling the real ones.

One extra dummy body was added to perform the role of the moving cart, with no geometry attributed.

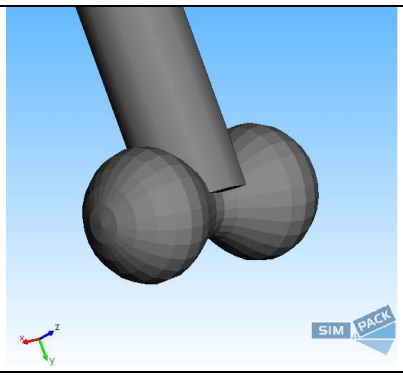

Figure 4.1 – Femoral Epiphysis

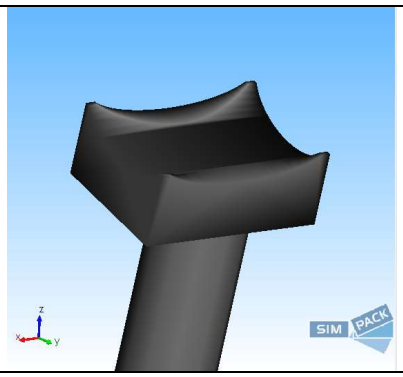

Figure 4.2 – Tibial Epiphysis

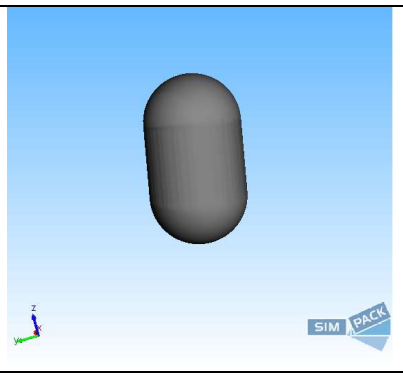

Figure 4.3 – Patellar component

4.1.2 Assembly and Constraints

The different bodies are then positioned in a 3D space [see Figure 30] and constraints are generated in correspondence of the distal and proximal epiphysis of respectively tibia and femur.

Both constraints are set as hinges, allowing revolution around x axis: the tibial one is referred to the Isys (Inertial System) and so has fixed coordinates, while the femoral one is set between the bone and the dummy body with the function of mobile cart.

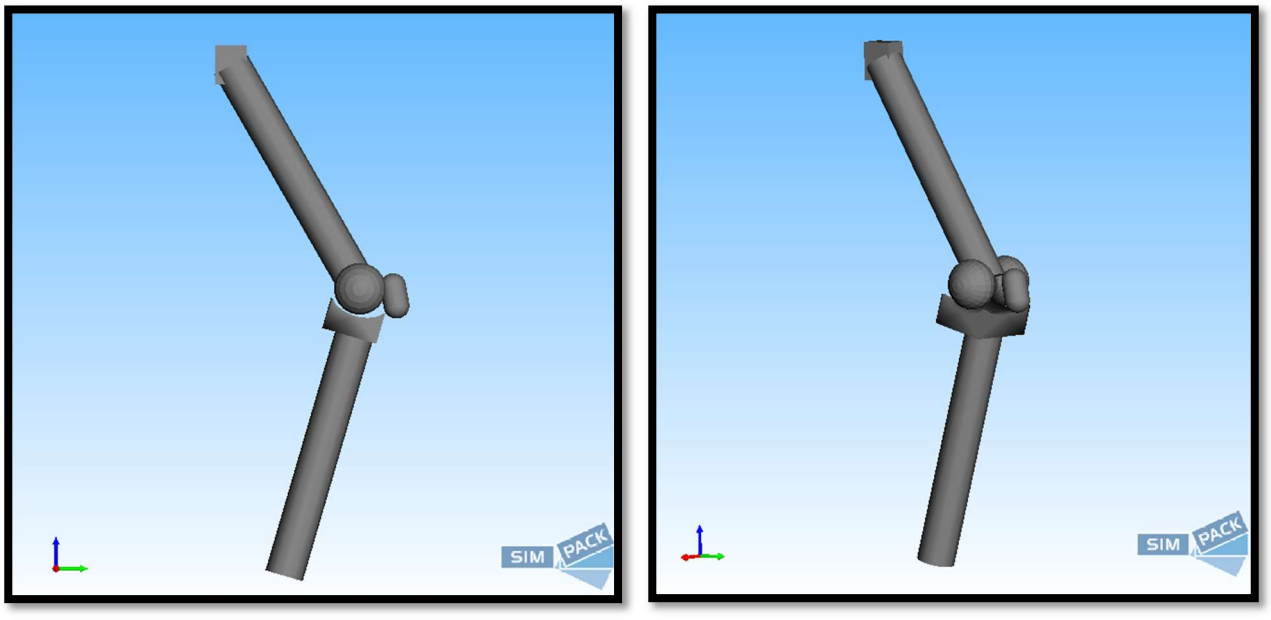

Figure 4.4 – The bone structure assembled

4.1.3 Forces

To simulate reactions among the different bodies, Contact Force Elements have been used to relate tibia, femur and patella and so mechanical properties of the materials involved were used as input.

"The Contact Force Element enables 3D multi-point contact between arbitrary surfaces. The surfaces are described by tessellated geometries, i.e. by polygon shells, or meshes, which gives the method the name 'Polygonal Contact Model' or 'PCM' [35]. The normal contact force is calculated using an 'elastic layer' model[36]. Additionally, the element calculates damping and friction forces."[37]

Then ligaments and tendon were then added, simulating them through "point-to-point" elastic forces (represented graphically by springs [see Figure 31]) [37].

Ligaments and tendons taken in consideration were:

- Lateral/Medial Collateral Ligament
- Anterior/Posterior Cruciate Ligament
- Patellar Tendon

It is to be noted that the dimensions of the geometries and the values of any mechanical property are far from the real ones, as they were chosen only aiming to an approximate visual result.

Point-to-point springs were used also to simulate muscles in this model, because the movement analyzed is passive and so the only force component they provide is the elastic one; to distinguish them from ligaments and tendons, they have been visually represented with polygonal geometries [see Figure 32], but this does not affect in any way the numeric results of the simulation.

The muscles considered in this model were then:

- Quadriceps
- Hamstrings

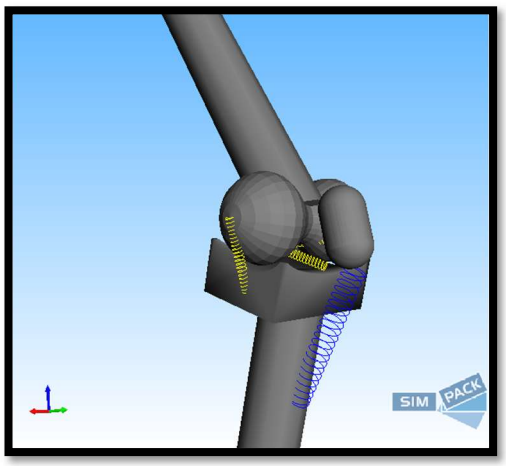

Figure 4.5 – Ligaments Representation

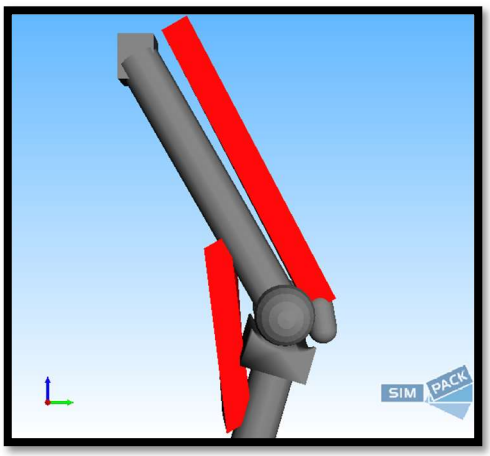

Figure 4.6 – Muscles Representation

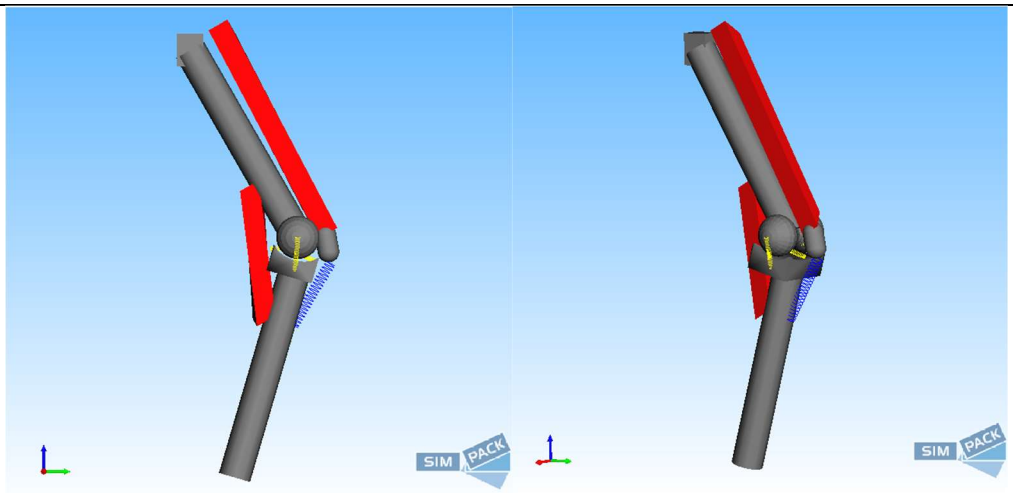

Figure 4.7 – The Model assembled

4.2 Second Model – Realistic Geometries

Having set the core model, the next step in the project is to reach a reasonable level of realism: new geometries are then taken in consideration.

4.2.1 Bodies and Geometries

To improve the fidelity of the reactions among bodies, a ".cae" file is then used to obtain the following geometries used to generate the respective bodies:

4.2.1.1 BONES GEOMETRIES AND LIGAMENTS INSERTION POINTS

The geometries imported already comprehended spherical markers to highlight the insertion points for the ligaments and centers of rotation, so those spheres were maintained in the import and used as reference [see Figure 34 - 35].

Table 1 – Bones Properties

Femur	Tibia
• Full volume • 375.1 g	• Full volume • 269.3 g

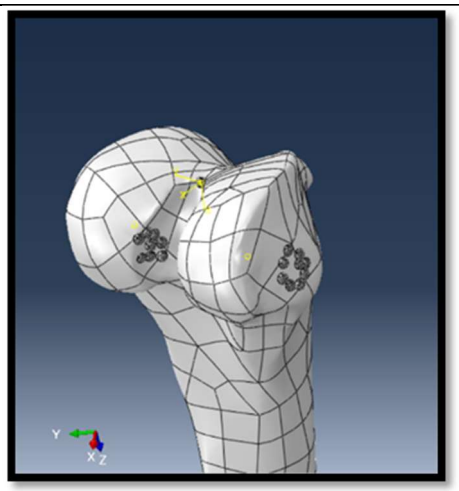

Figure 4.8 – Femoral Epiphysis

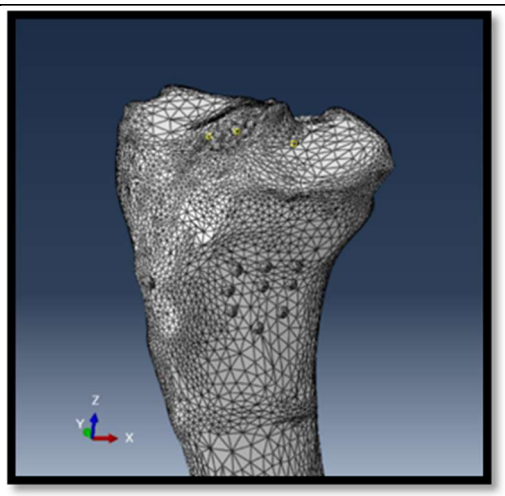

Figure 4.9 – Tibial Epiphysis

4.2.1.2 LINK'S "GEMINI" PROSTHESIS[38]

The chosen prosthesis is a PS (posterior stabilized) fixed bearing: this type of prosthesis contemplates the total removal of the cruciate ligaments, whose stabilization action is guaranteed by the post-cam system, and a rigid joint between the polyethylene insert and the underlying tibial plate.

Model and size have been chosen accordingly to the geometry of the native joint.

Table 2 – Prosthesis Features

Tibial Plateau	Tibial Insert	Femoral component
• Made in CoCrMo • 130 g mass • Third model • Size 7 • Type A • 5° posterior slope • 2 mm thickness	• Made in UHMWPE • 20 g mass • Third model • Type B • 6 mm thickness	• Made in CoCrMo • 250 g mass • Third model • Size 7

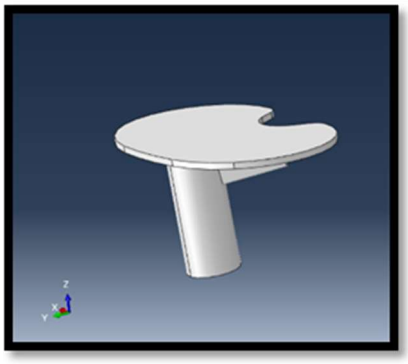

Figure 4.10 – Tibial Plateau

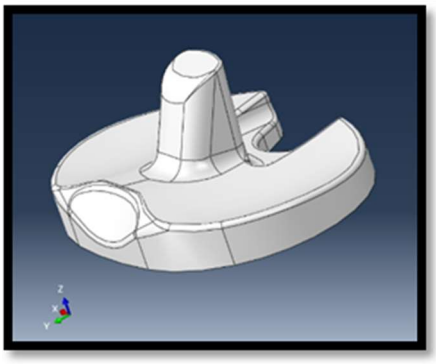

Figure 4.11 – Tibial Insert

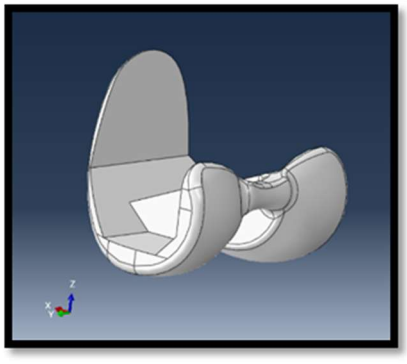

Figure 4.12 – Femoral Component

This last component was then split and partitioned to allow a more specific analysis of the contact forces between the polymer insert and the lateral [see Figure 39], medial [see Figure 40] and cam [see Figure 41] sections of the femoral part, otherwise considered as one and then less useful.

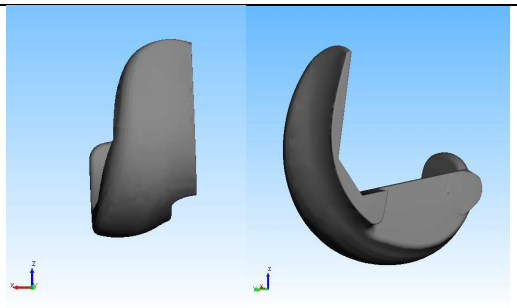

Figure 4.13 – Lateral Section

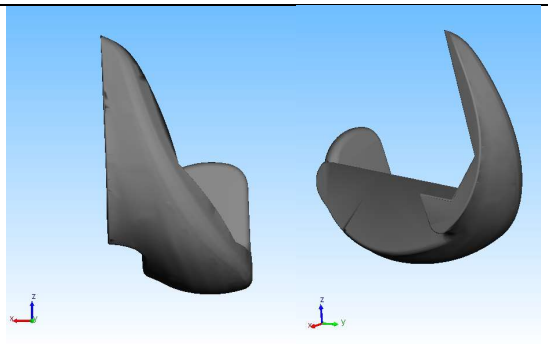

Figure 4.14 – Medial Section

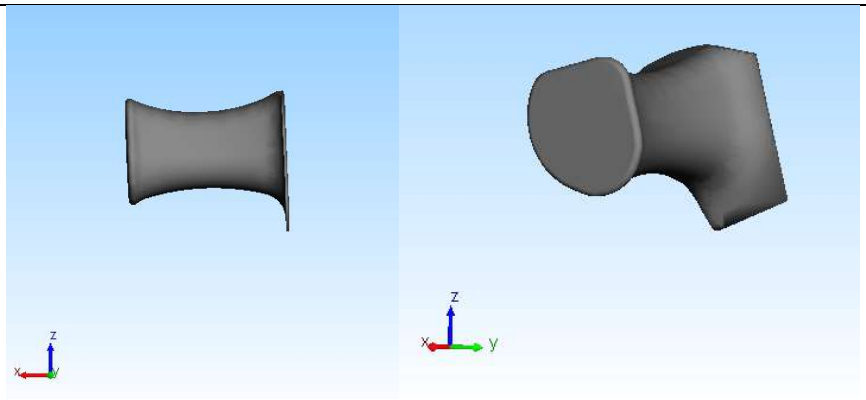

Figure 4.15 – Cam Section

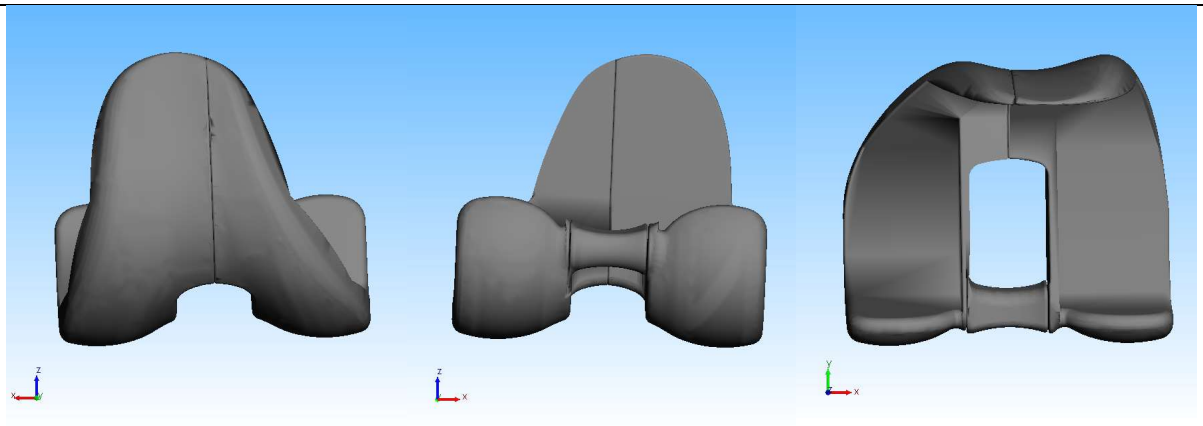

Figure 4.16 – Femoral Component assembled

4.2.1.3 Bones Cutting and Positioning

To assemble bones and prosthetic parts, a proper cutting is needed as it is during a real TKA operation[39].

Extruded cuts have then been applied to the bony geometries via ABAQUS [see Figure 43 - 44]; posterior referencing was adopted to perform the relative chirurgical techniques (avoiding in this way the possible changes in the joint line usually caused by anterior reference[39]) accordingly to the dimensions of the selected prosthesis.

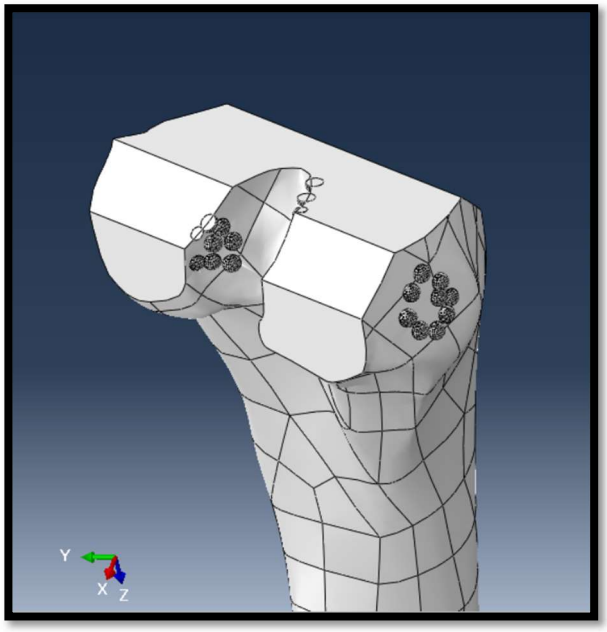

Figure 4.17 – Femoral Epiphysis Cut

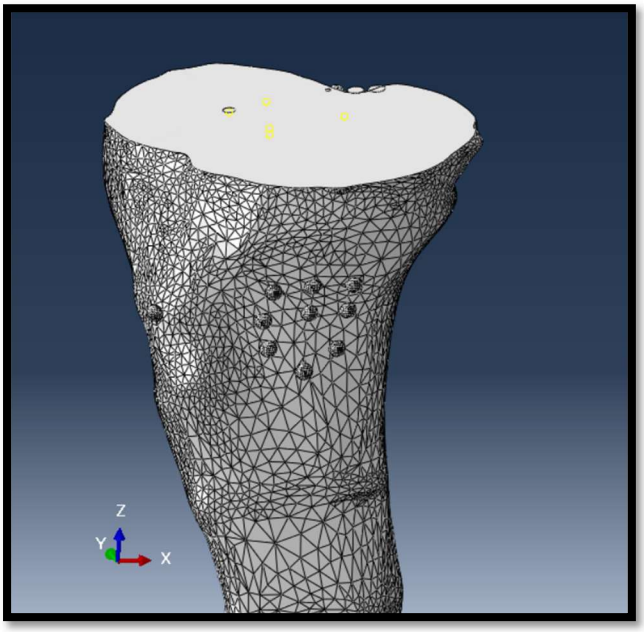

Figure 4.18 – Tibial Plateau Cut

4.2.2 Assembly and Constraints

The obtained parts were then imported on Simpack as body geometries for each considered body.

The prosthesis positioning on the modified joint has been executed following the chirurgical criteria, starting from the bone-prosthesis constraints and then working on the relative position of the structures constituting the joint [see Figure 45 – 46 – 47 – 48][58].

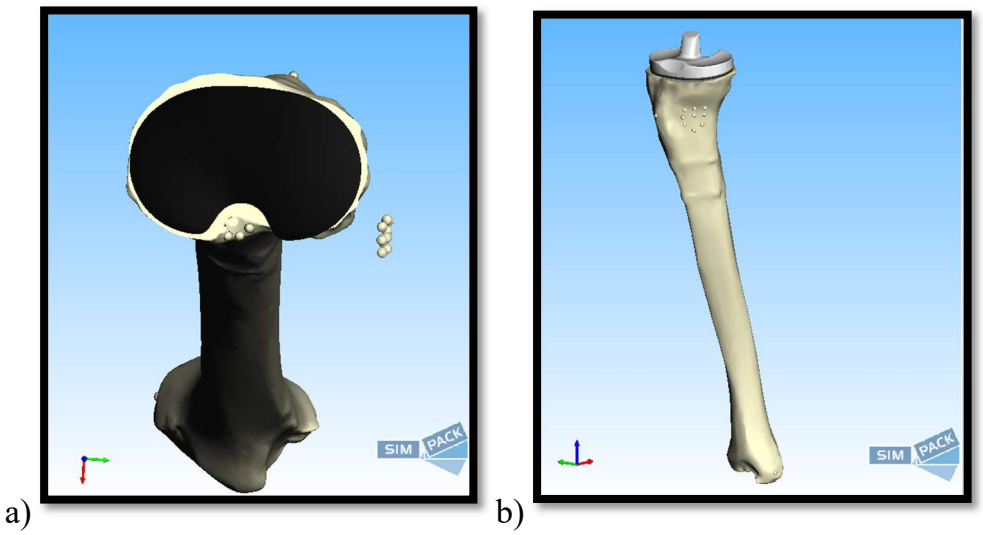

Figure 4.19 – Tibial Plateau (a) and Insert (b)

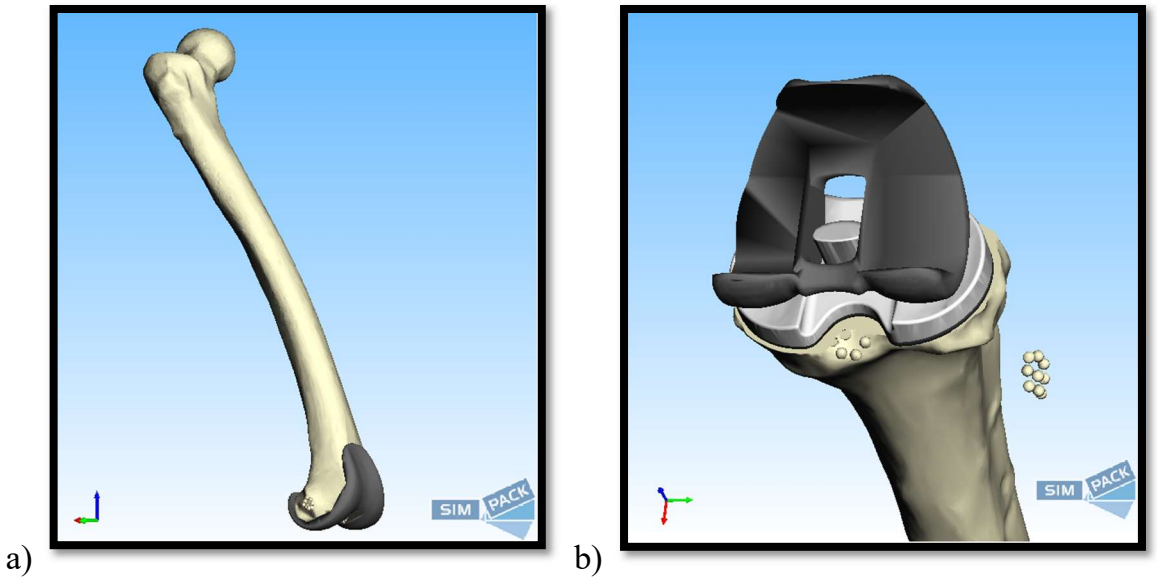

Figure 4.20 - Femoral Component, relative to Femur (a) and Tibial Insert (b)

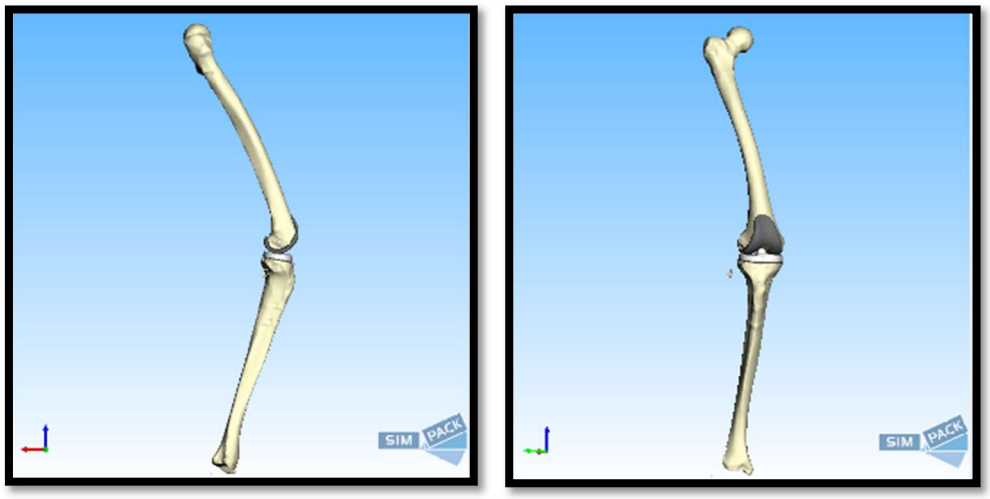

Figure 4.21 – The Model assembled

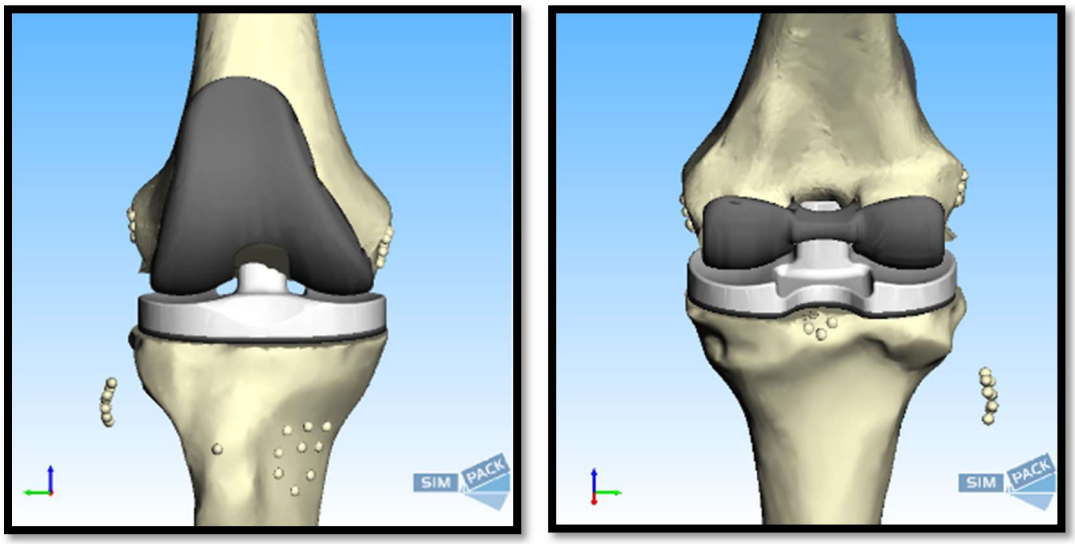

Figure 4.22 – Detail of the prosthetic implant

Relations among the joint and the virtual rig were set via constraints in correspondence of femoral and tibial rotation centres (the spherical markers present in the imported geometries) [see Figure 49]: tibial one was coupled with the rail and hence with the Isys itself, while femoral head was constrained to the moving cart. In this model tibial constraint was set as Spherical (meaning that any translational movement between selected points was locked, leaving nonetheless freedom to rotational movements[37]) while the joint between femur and cart allowed only rotation around the medio-lateral axis.

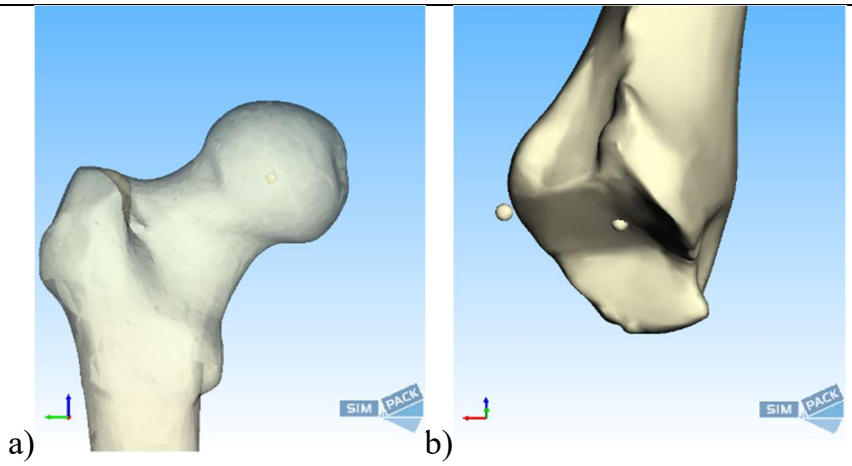

Figure 4.23 – Femoral (a) and Tibial (b) rotation centres

4.2.3 Forces

Being the rigid-body model of the limb assembled, it was possible to achieve a first simplified simulation in which only contacts between prosthetic parts and elastic force in the collateral ligaments were taken in consideration, ignoring thus muscles, patellar bone and its ligament.

Contact forces involved in the simulation are the same used in the previous model, here considered between the femoral component and the insert: this time realistic mechanical properties have been used for the components involved in the process, based on the materials used to produce the foretold parts[40] [see Table 3].

Table 3 – Prosthesis Mechanical Properties

Material	*Young's Modulus [MPa]*	*Poisson's Ratio*
CrCoMo	220000	0.3
UHMWPE	685	0.4

In order to recognize the collateral ligaments attachment sites, markers were generated in correspondence of the spherical geometries and an additional one was generated to represent the ideal union point of the different fibers [see Figure 50]; cylindrical deformable geometries were then used to visually represent the ligaments during the simulation [see Figure 51 – 52]. "Biomotion –Tendon" force element[37] was used for the ligaments, implementing their elastic and damping properties together with hysteresis effects[41] [see Table 4].

Table 4 – Ligaments Mechanical Properties

LIGAMENT	*Stiffness [N/mm]*
Lateral Collateral Ligament	19.5
Medial Collateral Ligament	21.4

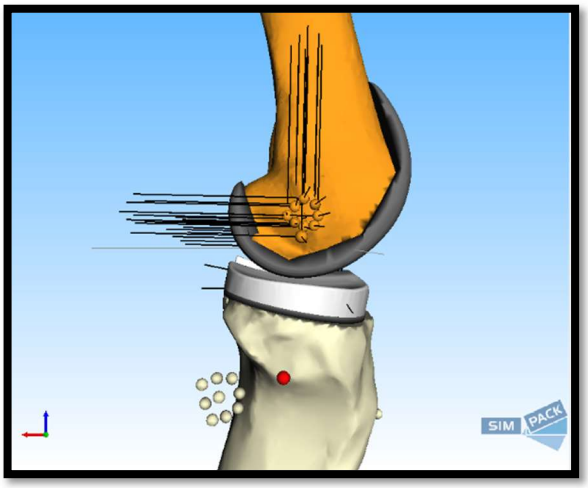

Figure 4.24 – Markers generated

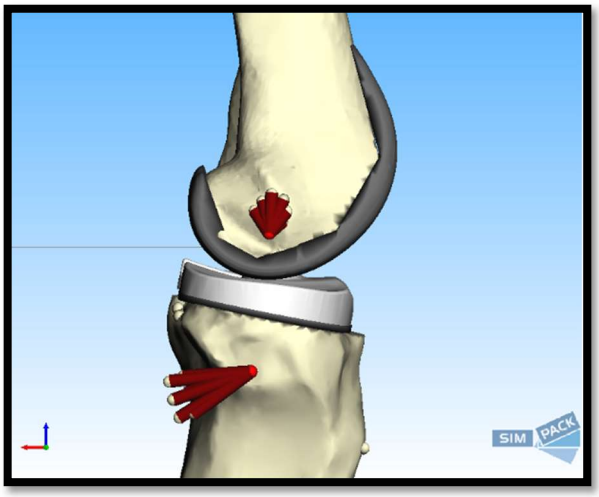

Figure 4.25 – Cylindrical bodies

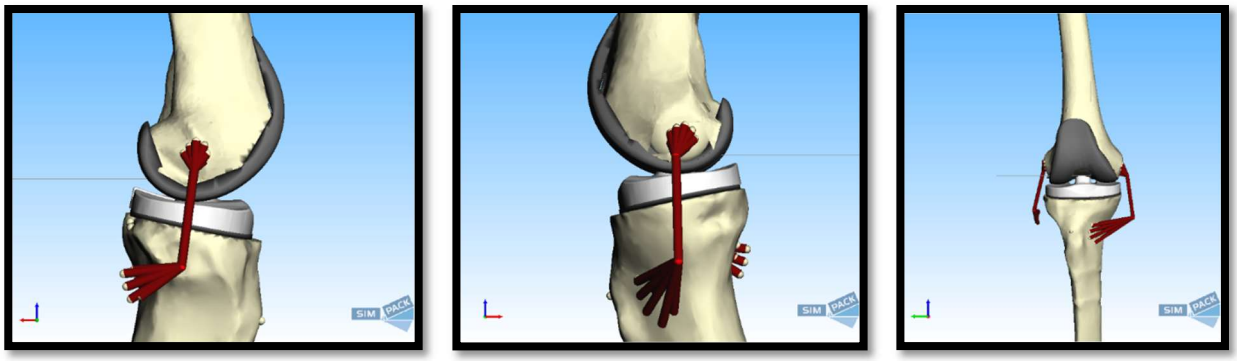

Figure 4.26 – Collateral ligament representation

4.3 Third Model – Patellar Component, Weak Tendon

Once obtained a structure based on real bones and prosthesis able to perform a primitive flexion-extension movement, the following element to be implemented with the purpose of obtaining useful results is the patellar system, comprising the muscles and ligaments connected to it.

4.3.1 Bodies and Geometries

Starting from the bodies in the previous model, a new prosthetic component is added to represent the patellar component [see Figure 49].

Patellar bone itself, to which the prosthesis would be fixed to, was not taken in consideration for the model as it had no influence on the contact relations involved.

Table 5 - Prosthesis features – Patellar component

Patellar component
• *Made in UHMWPE* • *28 mm diameter* • *10 g mass*

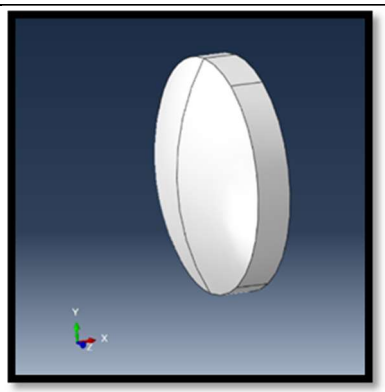

Figure 4.27 – The Patellar Component

Moreover, a new partition has been applied to the femoral component to allow its proper interaction with the patellar component, removing the splitting in the frontal area to avoid problems related to contact forces surfaces [see Figure 54 – 55 - 56].

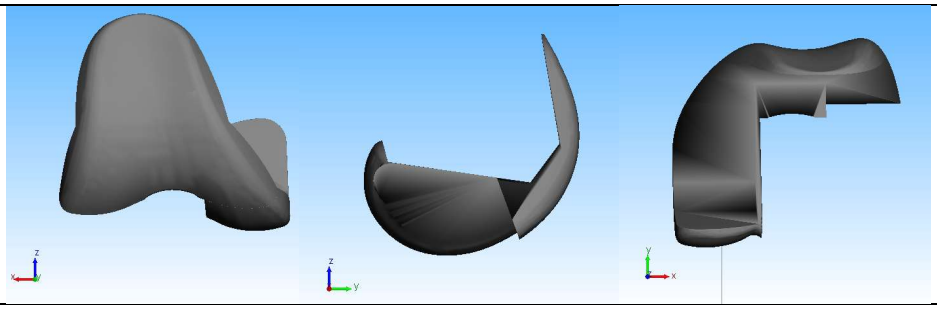

Figure 4.28 – Femoral Component, Medio-Frontal

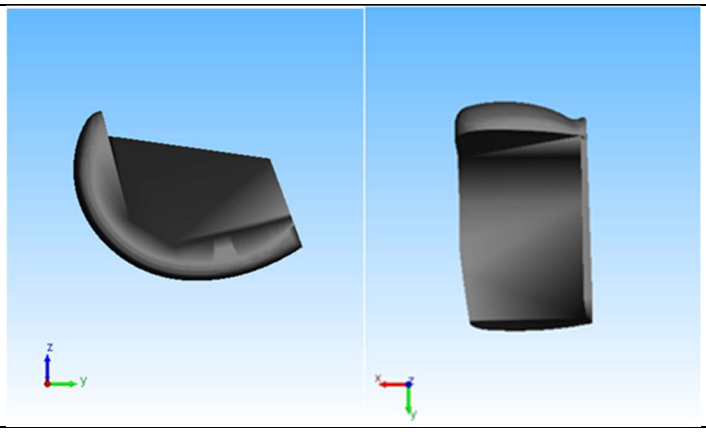

Figure 4.29 – Femoral Component, Lateral

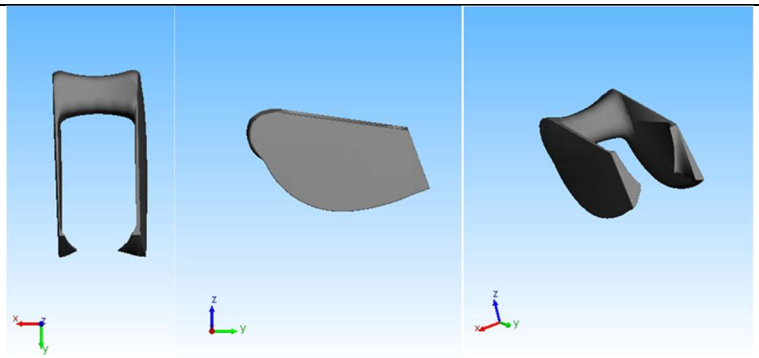

Figure 4.30 – Femoral Component, Cam

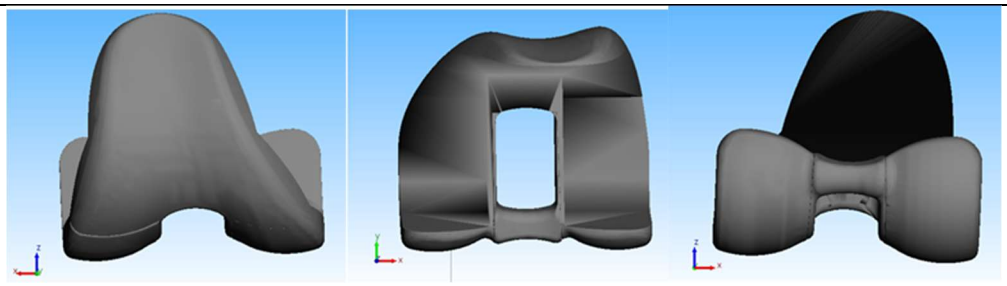

Figure 4.31 – Femoral Component, Assembled

4.3.2 Assembly and Constraints

An initial positioning of the patellar component was performed to evaluate the outcome of its addition to the previously tested model; the situation falls in a “patella alta” case [see Figure 58 - 59][72], but this pathology does not undermine the purpose of the current operation, which at this level is still a simple feasibility check.

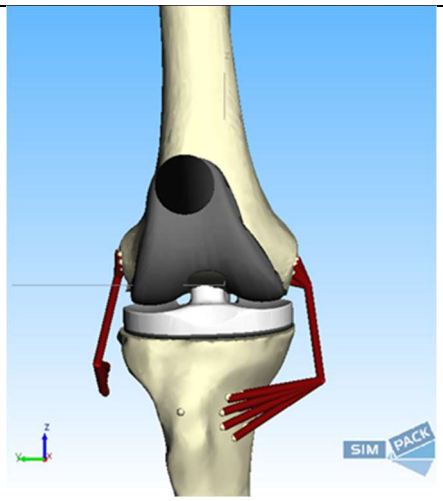

Figure 4.32 – Patellar positioning, front

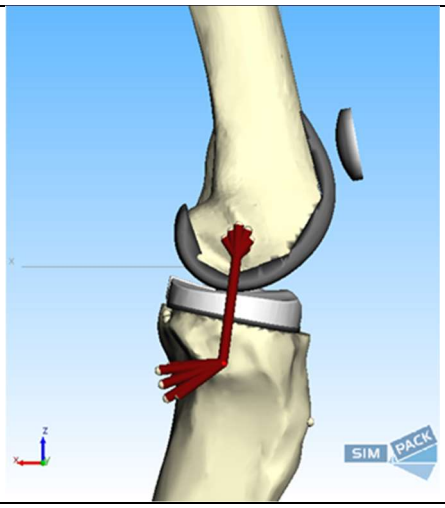

Figure 4.33 – Patellar positioning, lateral

4.3.3 Forces

The forces involved in this model, applied in addition to those already implemented in the previous one, have to cover the roles of quadriceps muscle and patellar ligament to allow the patella to perform its function in the movement.

The "Biomotion - Muscle / Tendon"[37] force elements were respectively used to represent those tissue contributions, acting between couples of user-defined markers: quadriceps were then modeled connecting the proximal end of the patellar component to a marker positioned proximally on the femur, in order to recreate simplistically the direction of action of these muscles; patellar ligament force element was instead imposed between the distal end of patellar component and the tibial tuberosity (represented as a spherical geometry [see Figure 58 -59]).

The values given as input to the force elements are shown in Tables 6 and 7 (which however have only a qualitative purpose as they have been changed arbitrarily during the completion of the model to reach acceptable results).

Table 6 - Muscle mechanical properties – Quadriceps

QUADRICEPS MUSCLE	
Area	47.9 [cm^2][42]
Stiffness	1000000 [N/m]

Table 7 - Patellar tendon mechanical properties

PATELLAR TENDON	
Stiffness	450 [N/m]

4.4 Fourth Model – Fixed Height of Patellar Component

The input provided to the previous model and the relationships between the different bodies have been changed in the "trial and error" process leading to the optimal solution.

4.4.1 Bodies and Geometries

No bodies or geometries have been added or modified.

4.4.2 Assembly and Constraints

Starting from the previous model layout, a new joint was added between the distal end of the patellar component and the tibial tuberosity to simulate the patellar ligament. This joint allows any form of rotation or medio-lateral and anterior-posterior displacement but prevents proximo-distal translations between the two markers, in order to avoid the excessive rising of the patella spotted with the previous configuration.

4.4.3 Forces

The forces applied are the same as in the previous case with the exception of the one simulating the patellar ligament, which was initially replaced by the above-mentioned translational constraint on its own; it was then reintegrated so as to have the effect of the ligament elasticity in the medio-lateral and antero-posterior directions, but keeping a rigid constraint in the proximo-distal one.

4.5 Fifth Model – Hollow Bones and Patellar Ligament

The following step is then finding an effective modeling method for the patellar tendon, which unlike in previous models should also perform the wrapping effect; this need can be fulfilled applying a series of contact forces among the newly implemented tendon bodies and the prosthetic ones already present.

To improve the model before moving on to the insertion of the patellar tendon bodies, anyway, bony geometries need to be changed to take into account the different distribution of their whole mass between cortical and cancellous bone: if in the previous models those bodies were considered as full volumes (in which the mass was uniformly distributed), now the bones are represented by the cortical tissue only (as it is considered to be the bone component actually influencing the location of the center of gravity).

4.5.1 Bodies and Geometries

Tibia [see Figure 60] and femur [see Figure 61] were then imported from another file in order to obtain geometries with hollow structures; the surgical cuts necessary for the positioning of the prosthesis were again performed following the same guidelines used previously, going then to cover the opened epiphysis with thin flat surfaces and finally smoothing the sharp edges to avoid problems in the calculation of the contact forces.

The same masses applied previously were used to characterize these bodies [see Table 1].

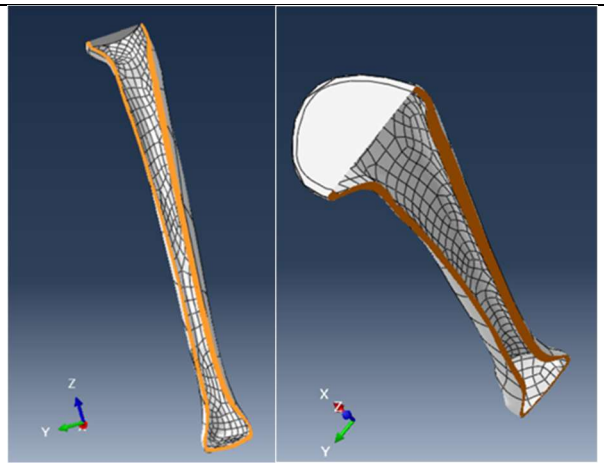

Figure 4.34 – Hollow Tibia Section

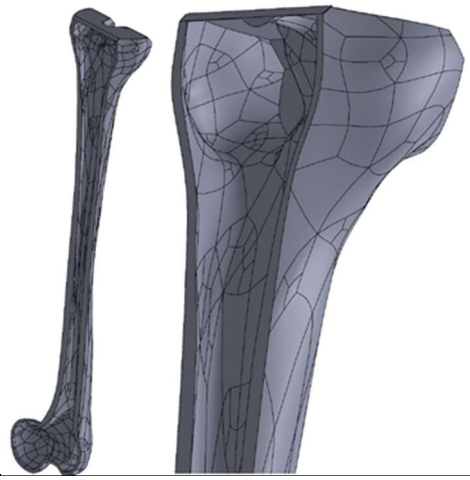

Figure 4.35 – Hollow Femur Section

4.5.2 Assembly and Constraints

The positioning in the virtual environment of the new bone geometries and prosthesis has been performed with the same technique employed for the other models, whilst more effort was involved in determining the attachment points for the collateral ligaments and in the modeling of the patellar one.

4.5.2.1 Collateral Ligaments

The imported bone geometries, in fact, do not report the attachment points for ligaments as in the previous ones, and for this reason markers were generated on each body [see Figure 62 - 63] following literature studies[43,44,45].

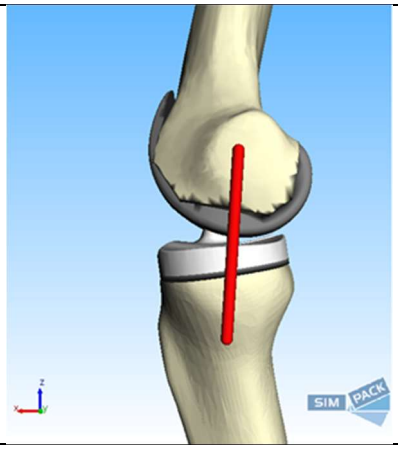

Figure 4.36 – Medial Collateral Ligament

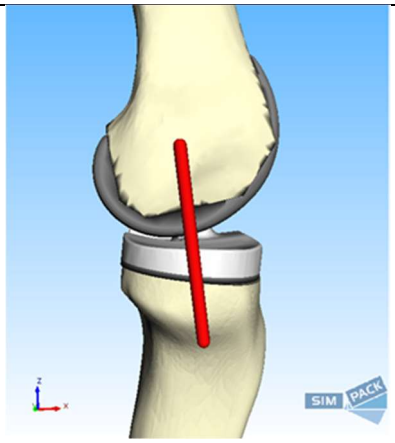

Figure 4.37 – Lateral Collateral Ligament

4.5.2.2 Patellar Ligament

Patellar component is the next scope to improve: the sought-after wrapping effect can be achieved by implementing bodies and interconnecting them with the supporting structure, so different possibilities have been examined to reach an optimized one.

I. Parallelepiped

The first attempt was made by imposing a rectangular geometry in order to have a sufficiently large contact area; however, the concept of tendon flexibility is missing, and therefore the solution does not reflect the needs thus it has been discarded. [see Figure 64]

II. Cylinder array

To simulate the flexibility of the ligament, an array of cylinders connected to each other by spherical constraints is generated. This ideally optimal solution, however, leads to an excessive increase in computation time, so it has been discarded for the sake of a faster one. [see Figure 65]

III. Modular Cylinder

To avoid using the array but still maintain the concept of modularity to simulate the bending of the ligament, a column of cylinders constrained to their extremities is implemented and this solution turned out to be optimal, even if using only one column fails to properly render the wrapping effect with surrounding elements. [see Figure 66]

IV. Multiple Modular Cylinder

To improve the effects of wrapping, three different columns of cylinders have been implemented; central elements in each assembled cylinder is then modelled as an ellipsoid to guarantee a smoother contact surface and avoid sharp edges. With this layout, contact is guaranteed for greater area and the yield improves, thus bringing the solution to be adopted as the final one. [see Figure 67]

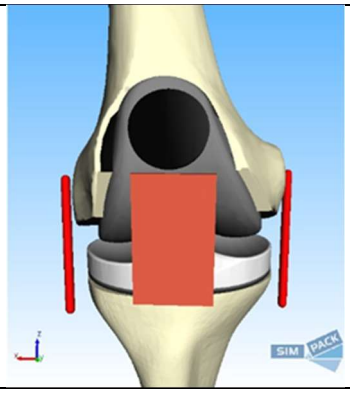

Figure 4.38 - Parallelepiped

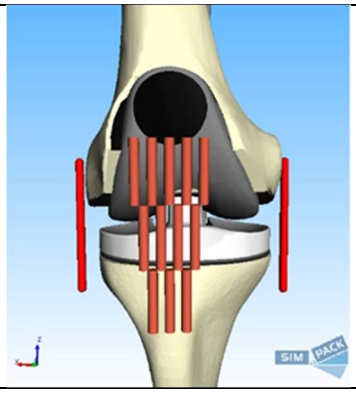

Figure 4.39 - Cylinder array

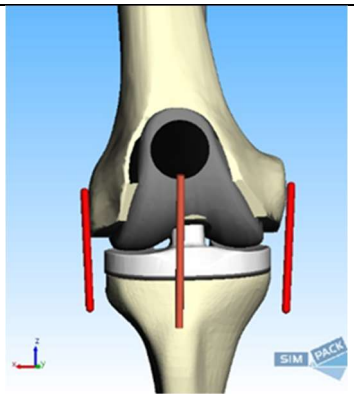

Figure 4.40 - Modular Cylinder

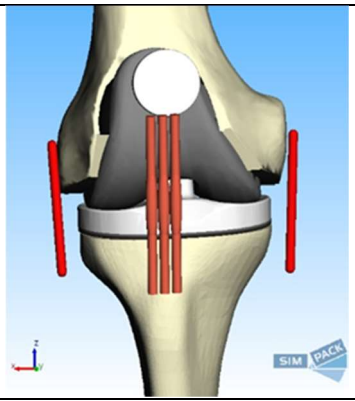

Figure 4.41 - Multiple Modular Cylinder

4.5.3 Forces

In the various trials performed to find the most suitable model for the patellar ligament, the forces used were Contact and Muscle-Tendon ones[37].

Contact forces utilized were the same as those previously applied, with the addition of those regarding the interaction between the prosthesis and the patellar ligament whose geometries were considered totally rigid. For what concerns muscular and ligamentous forces, the data reported in the Tables 8 and 9 have been taken as a reference and have been used in different ways, firstly applying a single force and then splitting the total value in different branches to analyze in a more realistic way the action of the soft tissues involved.

In the final model [see Figure 67], the quadriceps muscle is connected with three heads to the prosthetic patella, in turn connected to the three branches of the patellar ligament and consequently to the tibial tuberosity through tripartite forces (and therefore with eventually modified properties).

Table 8 - Muscle mechanical properties – Quadriceps

QUADRICEPS MUSCLE	
Area	40.8 [cm^2][42]
Stiffness	2147.36 [N/mm][47]
Damping	49.05 [Ns/m][48]

Table 9 - Patellar tendon mechanical properties

PATELLAR TENDON	
Stiffness	430.92 [N/mm][49]
Damping	40 [Ns/m] [50]

4.6 Sixth Model – Patellar rotation

Previous model, albeit its simplistic limits, has yielded interesting results and therefore has been enhanced by adding other components.

The major inaccuracy found previously was an excessive rotation of the patellar component around the mid-lateral axis during the flexed phase; this outcome was due to the fact that the quadriceps forces acted on the straight line linking the patella to the muscle related markers on the femur, and during the movement this line could therefore fall into the femur itself, leading to the generation of non-physiological forces and thus not corresponding to reality.

Various approaches have been adopted to overcome this problem, through the addition of bodies and contacts or with the use of forces and constraints.

4.6.1 Bodies and Geometries

1. **Quadriceps Body Contact**

The first approach consisted in employing a body to simulate the contact forces between the bone and the muscle, thus preventing the aforesaid non-physiological forces on the patella. An ellipsoid with a major axis lying on the line connecting the femoral marker with the patella [see Figure 68] has therefore been implemented together with the relative contact forces, but this addition has significantly increased the computation times and brought a series of inaccuracies and errors due to the non-rigorous representation of the soft tissue. Therefore, it was preferred to change approach, moving to impositions of constraints and forces rather than to contact interactions between bodies.

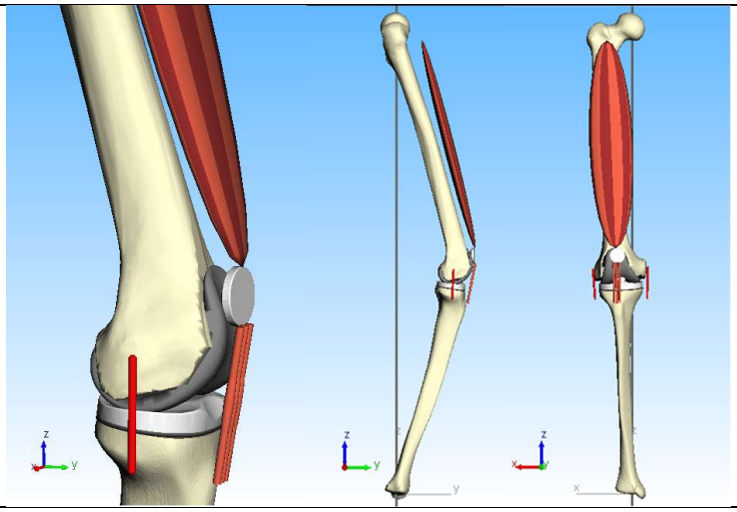

Figure 4.42 – Muscle Representation as a Body

2. 3D line constraint

The following attempt was then to implement a 3d curve parallel to the mechanical axis of the femur, coinciding with the muscular force direction in the beginning of the movement [see Figure 69]. This curve was then imposed to be in solidarity with the femur, and a mobile body was implemented and constrained to it by a point-to-curve[37] allowing this way a sliding movement along the line.

This point-like body is nothing but a massless marker, from which are conducted the two forces in which the quadriceps action has been divided: the proximal force will always lye on the 3d curve inasmuch connecting the femoral marker with the intermediate body, while distally it will connect this latter with the patellar component preventing any form of force resulting on the prosthetic component to be directed posteriorly.

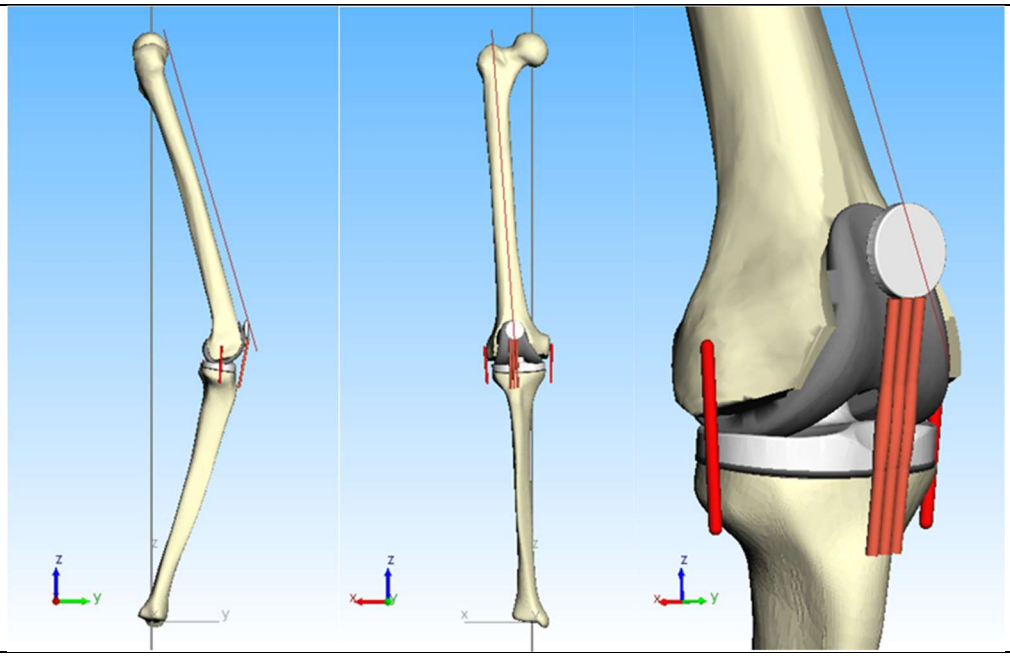

Figure 4.43 – Quadriceps 3D Curve

3. Additional bodies

The latter attempt, failed because of the excessive computing time, was followed by another one in which the intermediate point-like body switched to a bulky one by giving it a specific geometry: the strength of the quadriceps was therefore expressed only along the 3D line, while between the intermediate body and the patella a spherical constraint is imposed [see Figure 70]. The same technique has been enhanced by adding two further lines parallel to the first one and with their respective intermediate bodies in order to tripart the muscle force as previously done [see Figure 71].

This kind of constraint has however led to different complications that prevented a correct simulation of the flexion-extension and therefore the point-to-line method has been abandoned in favour of different strategies.

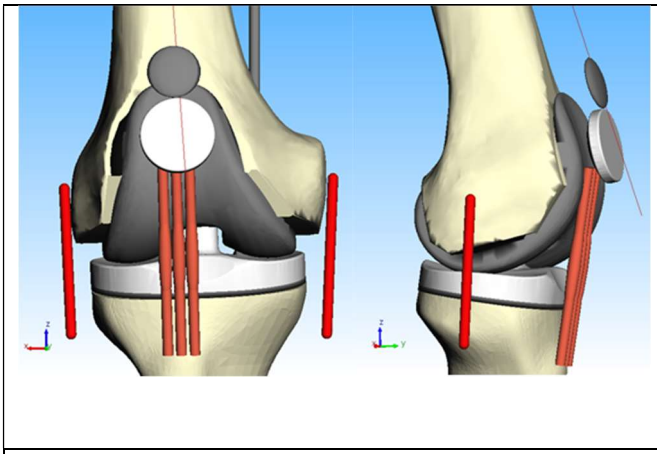

Figure 4.44 – Additional Body and 3D Curve

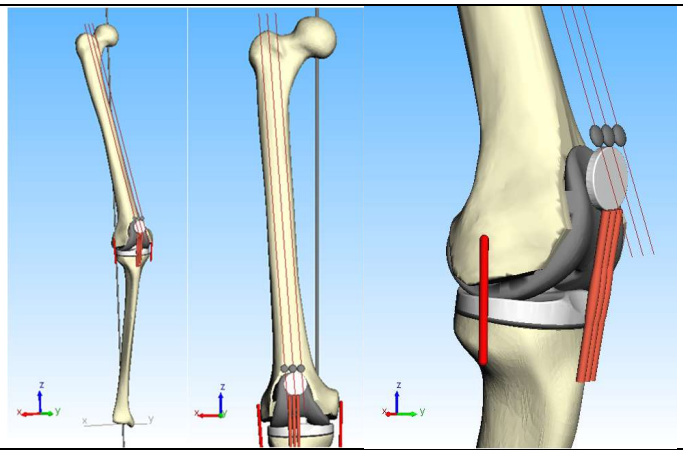

Figure 4.45 – Tripartition of the Quadriceps

4. Additional Patellar Geometry

Utterly changing the principle, a parallelepiped was applied to the patellar component [see Figure 72] in such a way that, thanks to its interaction with the femoral component, the excessive rotation movement previously found was eliminated; the main goal was reached in this way, but it actually isn't a reproduction of any real phenomenon so a different solution needs to be found.

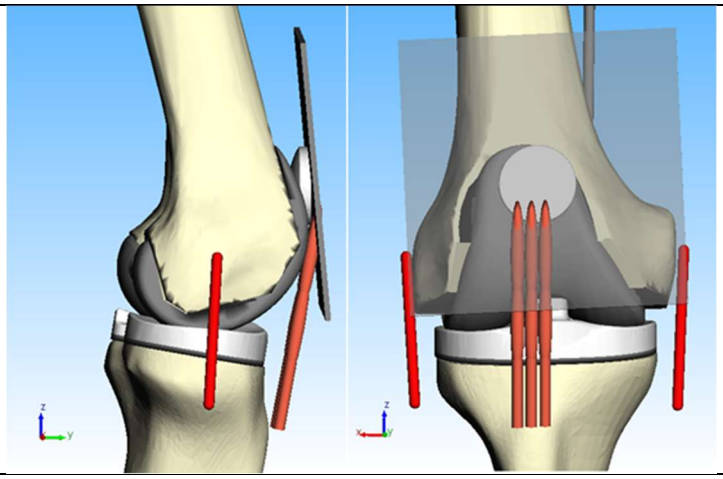

Figure 4.46 – The Parallelepiped Applied

5. Axial fixation forces

The option adopted as the final one implied the introduction of a unilateral forces[37] system able to reproduce the previously sought 3d curve methodology this time without the application of constraints on the line. The patellar component is therefore furnished with three attachment points for the quadriceps forces and three more for the patellar tendon, and an additional marker was implemented in order to be subjected to forces reacting to shifts of the proximal extremity from the quadriceps action line [see Figure 73].

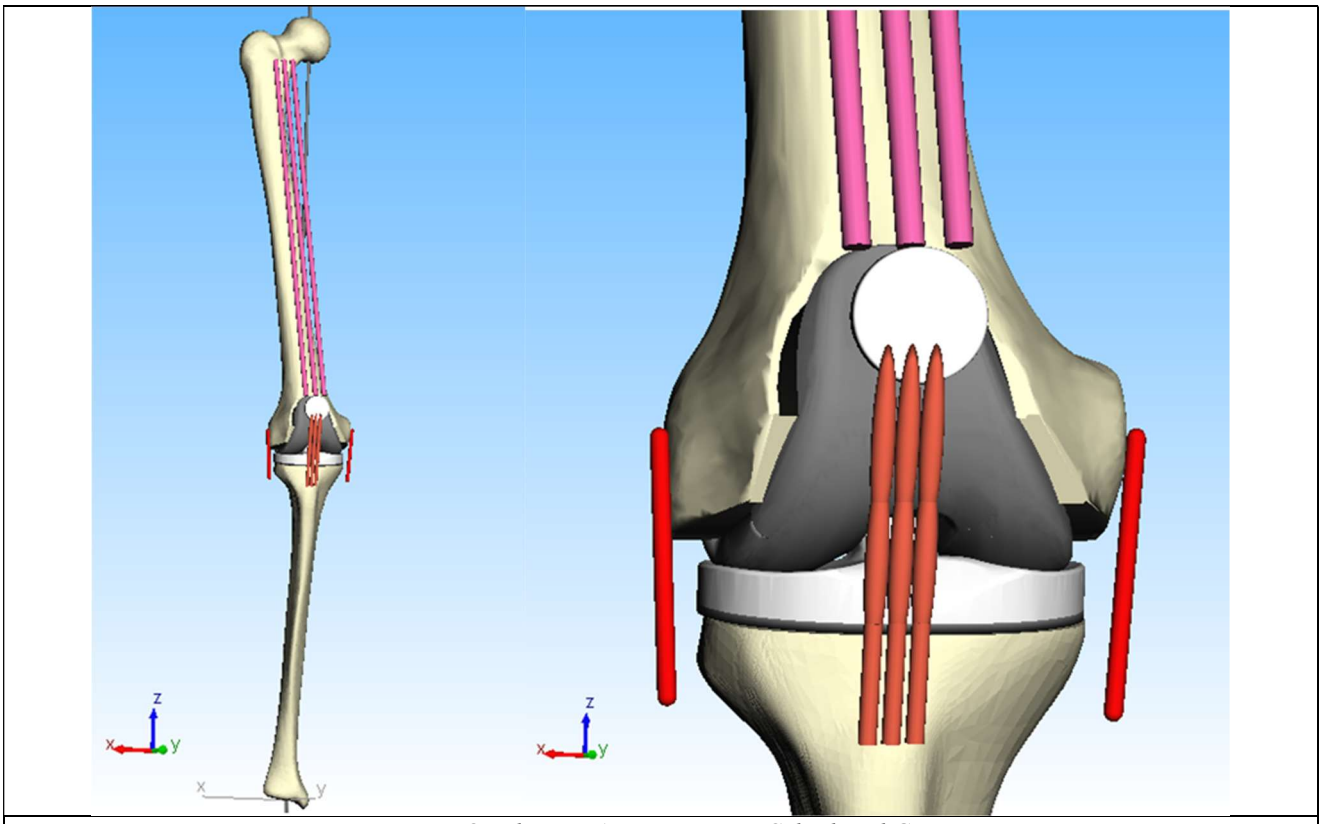

Figure 4.47 – Quadriceps Action Lines as Cylindrical Geometries

4.7 Seventh Model – MPFL and Lateral Retinaculum

Lastly, the effects of MPFL and lateral retinaculum were taken in consideration and added to the model; quadriceps force has also been taken in consideration to verify if the one obtained through simulation matches with the one already studied in literature.

4.7.1 Bodies and Geometries

Bodies adopted are the same used in the previous model, with the addition of two cylindrical geometries representing the aforesaid ligaments; their purpose is solely graphical, as they don't interact with any other body [see Figure 74].

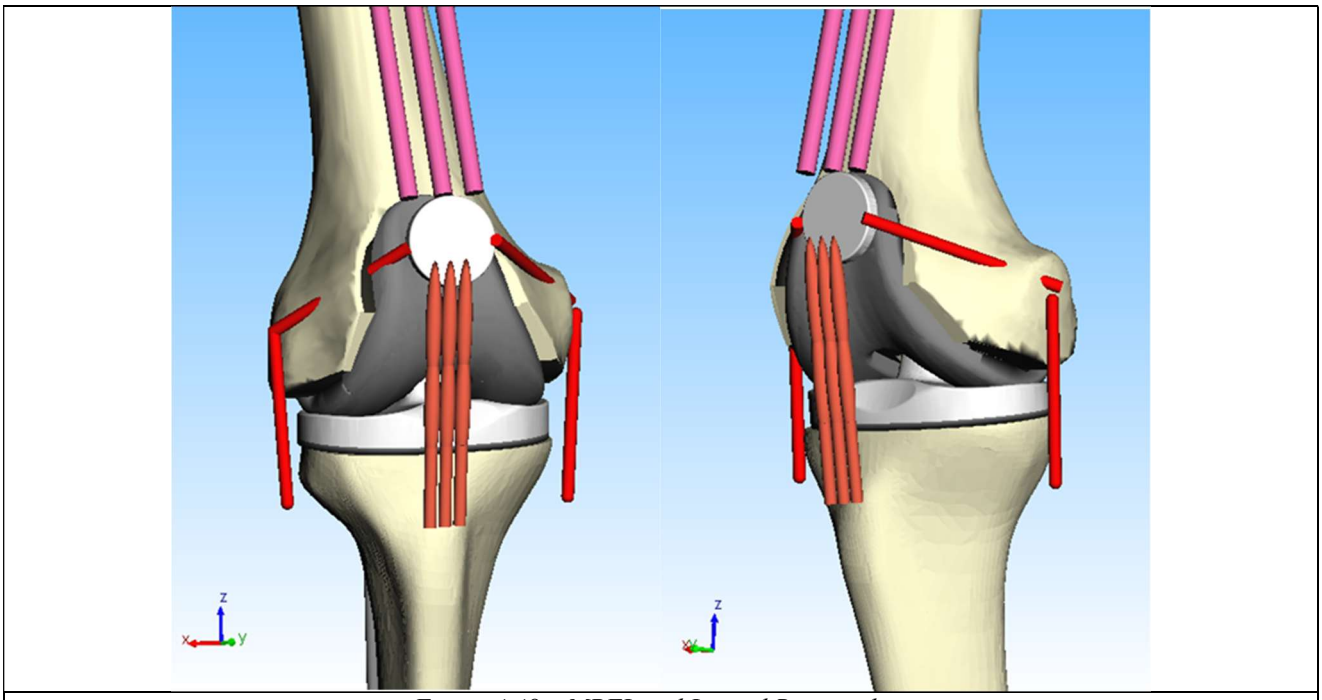

Figure 4.48 – MPFL and Lateral Retinaculum

4.7.2 Assembly and Constraints

No changes have been implemented from the previous model.

4.7.3 Forces

To simulate the contribution of MPFL and lateral retinaculum, a system of unilateral forces (similar to the one adopted previously, but this time acting on the medio-lateral direction) has been applied to the prossimal and distal extremities of the patellar component.

The values referring stiffness attributed to these forces are represented in Table 10 .

Table 10 - Patellar ligaments mechanical properties

PATELLAR LIGAMENTS	***Stiffness***
MPFL	29.38 [N/mm][51]
Lateral Retinaculum	16 [N/mm] [52]

5. Results

The simulations performed on the models, described in the previous chapter, have returned as output an abundant amount of data concerning the various aspects of the system movement and the relationships between the various bodies involved. Among these data, those that were taken into consideration and analyzed with particular attention were the ones concerning the contact forces between the various prosthetic components and the displacement relative to femoral and tibial epiphysis, which were used as an indication of the correctness of the model and consequently to understand how to improve it step by step.

5.1 First Model – Oversimplified

The animation obtained after the simulation is still inaccurate and patellar movements are heavily unrealistic, but the joint is able to perform a flexion-extension movement [see Figure 75] without returning errors or breaking and thus this model can be considered the first step to develop a better one.

Numerical results were ignored as they heavily depend on the mechanical properties attributed to the bodies, which in this model were totally unrealistic and so not to be taken in consideration.

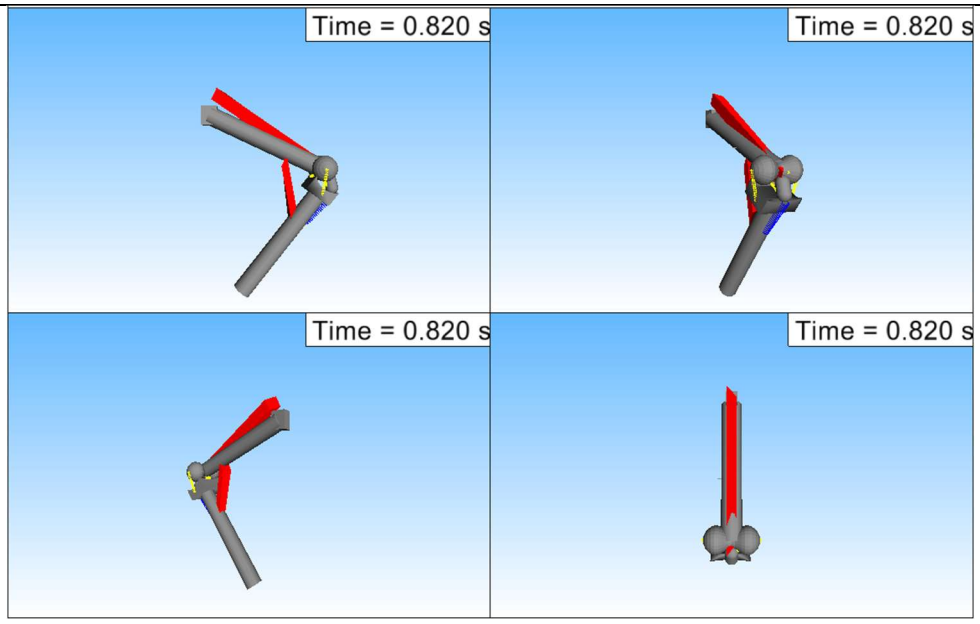

Figure 5.1 – A frame of the Animation obtained as an output

5.2 Second Model – Realistic Geometries

This model is mainly aimed at the visualization of possible problems in the movement and in the contact forces in a situation with realistic geometries; nevertheless, it has returned as output interesting contact forces and displacements as they are related to a knee joint without the patellar component.

The contact forces between the femoral component and the insert are not optimally distributed between the medial and the lateral sections, the latter being practically unloaded for the most part of the flexion resulting in a medial stress much higher than the physiological; moreover, the flexion angles of start and end contact in the post-cam mechanism are asymmetrical between flexion and extension due to the lack of patellar forces.

Regarding displacements and rotations, the results obtained fall within the range of possible movements but there are still errors and inaccuracies resulting from the absence of the patella: the extension movement in fact leads to a different relative position between the two bony ends than the starting one for what regards the intra extra rotation and the displacement along the anteroposterior axis, and this is mainly to be attributed to the lack of frontal pression.

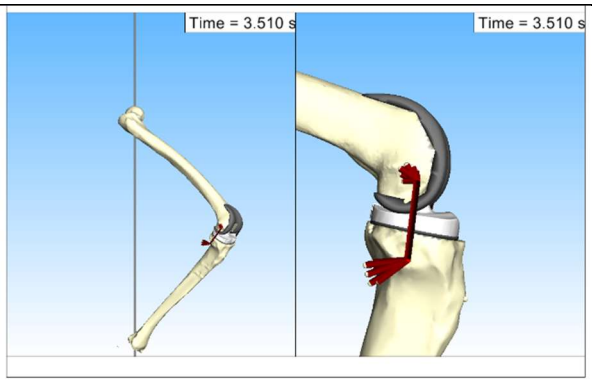

Figure 5.2 – Second model animation, lateral view

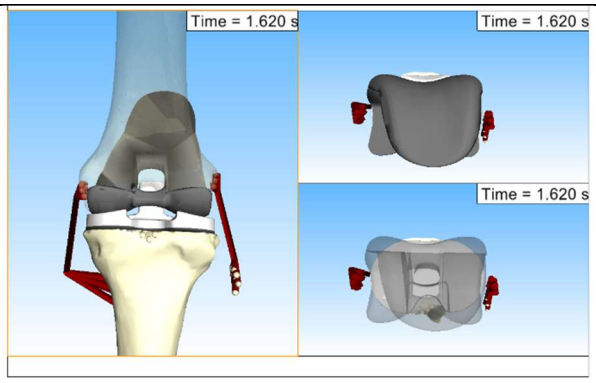

Figure 5.3 – Second model animation, back and top views

5.3 Third Model – Patellar Component, Weak Tendon

In this model, quadriceps and patellar ligament were defined only by a couple of markers each, and this led to unrealistic results; the main goal was although to set correctly the contact forces between patellar and femoral components, so the most useful outputs were not quantitative but qualitative and graphic results.

The presence of the patella was not able to excessively improve the results if compared to the previous ones, since the patellar tendon adopted in this case was not able to oppose the due resistance during flexion; therefore this resulted in the prosthetic part remaining almost attached to the femoral component surface without sliding and thus not exercising its role in flexion.

Medial force is comparable to the previous one and also in this case the lateral component appears to be almost unloaded for the whole movement, except for some peaks lacking significance anyway. The post cam system returns again an antisymmetric behaviour for what concerns flexion at contact starting and ending.

The addition of the patellar component also makes it possible to extrapolate the contact forces between the latter and the femoral component, which results to have a maximum at the moment of maximum flexion [see Figure 78].

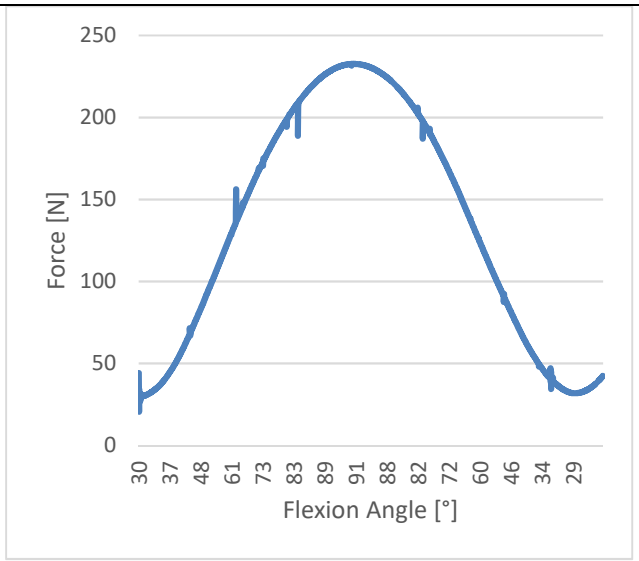

Figure 5.4 – Patello-Femoral Contact Forces

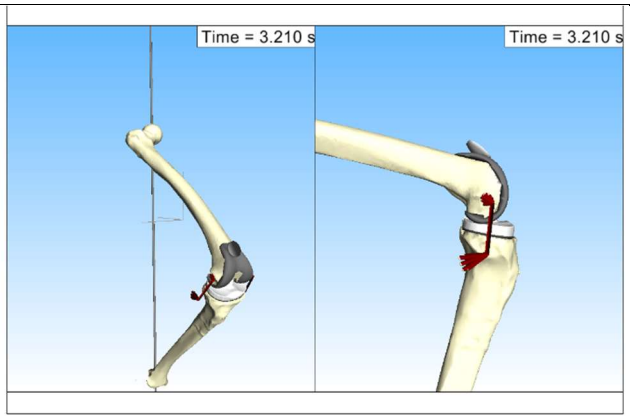

Figure 5.5 - Third model animation, lateral view

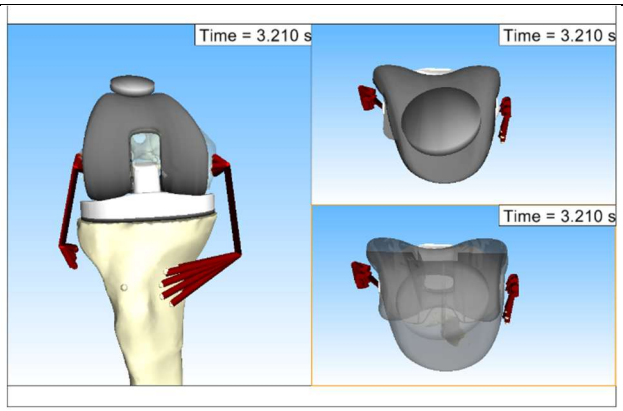

Figure 5.6 -Third model animation, front and top views

5.4 Fourth Model – Fixed Height of Patellar Component

Compared to the previous model, the displacement and the rotations found are in the same range and present a similar trend; contact force outputs instead returned higher values than the previous model but maintained the same trend [see Figure 83 – 84 – 85], while lateral ones showed to be still affected by instability and thus not significant.

However, the constraints imposed in this model do not reflect the real joint mechanics and therefore cannot be considered a good starting point for further developments.

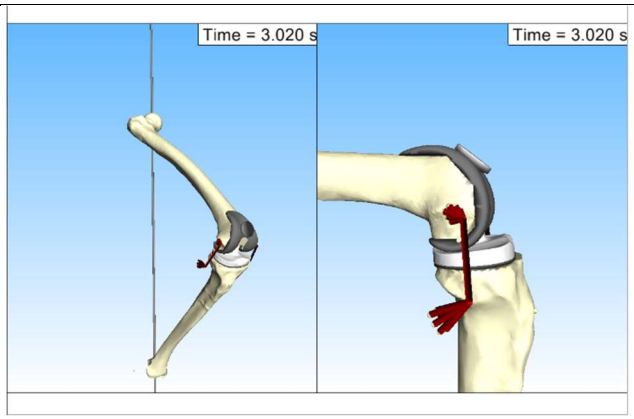

Figure 5.7 - Fourth model animation, lateral view

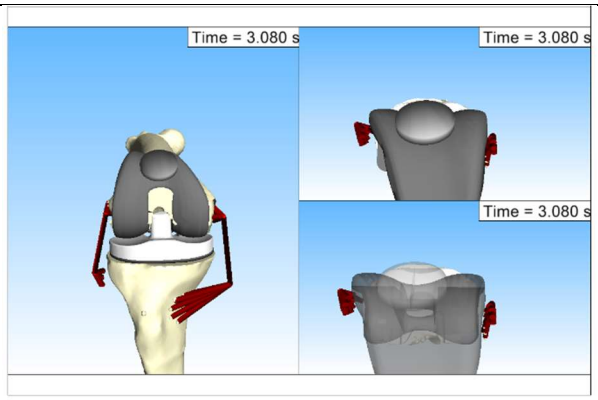

Figure 5.8 - Fourth model animation, front and top views

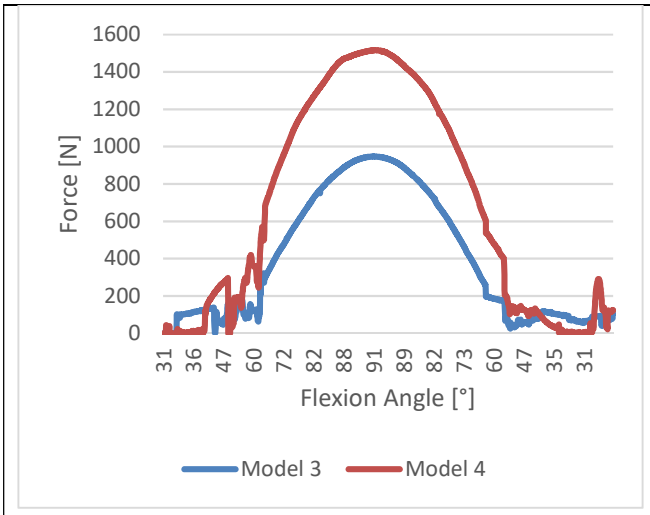

Figure 5.9 – Tibio-Femoral Contact Forces, Medial

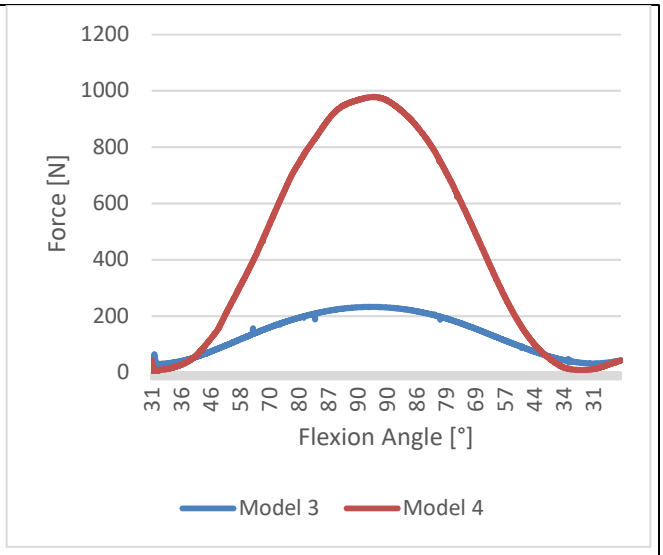

Figure 5.10 – Patello-Femoral Contact Forces

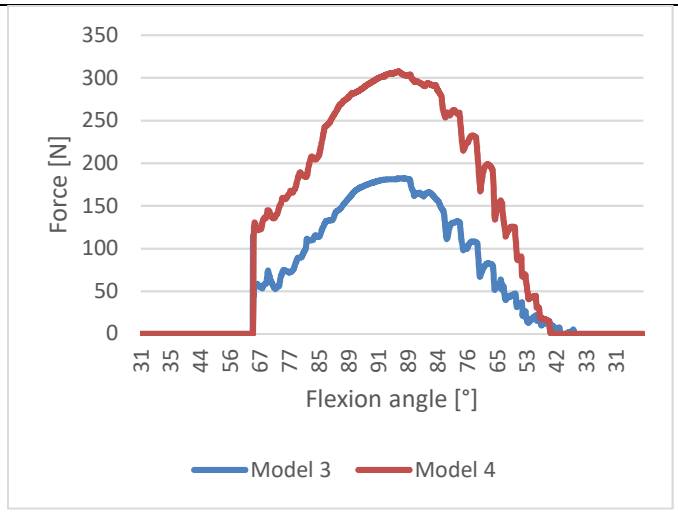

Figure 5.11 – Post-Cam Contact Forces

5.5 Fifth Model – Hollow Bones and Patellar Ligament

The addition of the patellar tendon as a set of bodies with surfaces and mass allowed to simulate the physiological wrapping effect and to reach better realism of the model, as reflected by the quantitative results although they still need to be refined.

The distribution of the contact forces between the medial and the lateral condyles still shows some incorrectness in terms of trend and values, and the post-cam system contact results to be happening for a flexion range larger than expected.

The patellar component then shows an anomalous rotational behavior on the mediolateral axis: this is a symptom of muscle or tendon forces modeling problems, and therefore implies a change of the way these latter have been implemented.

5.6 Sixth Model – Patellar rotation

Considering the first approach, although the visual result of the animation may seem to satisfy the predetermined objective, it is evident that this solution can be considered a stretch of the model and consequently the numerical outputs are still not acceptable for what regards trends and ranges [see Figure 86 – 87 – 88, in blue].

The likely values start to be reached with the second variant: the trend of the medial and lateral contact forces turns out to be sinusoidal in both sides and higher maximum is found in the medial sector; the contact in the post-cam system results then to be in the range of the physiological flexion angles and the magnitude of patellofemoral forces increases [see Figure 86 – 87 – 88, in red].

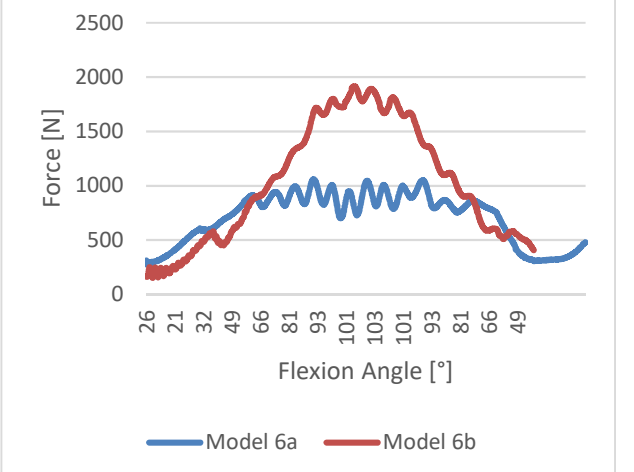

Figure 5.12 - Tibio-Femoral Contact Forces, Medial

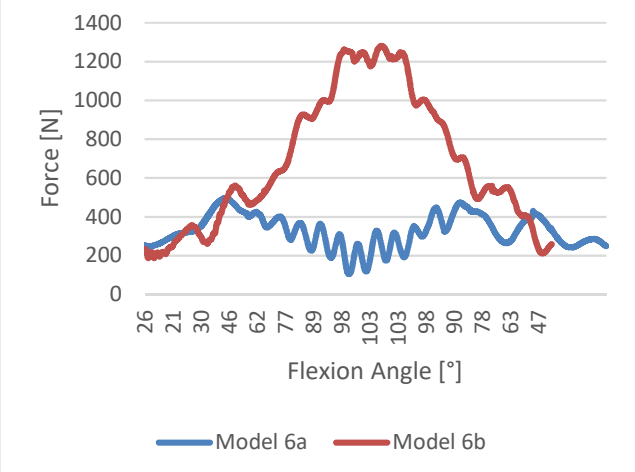

Figure 5.13 - Tibio-Femoral Contact Forces, Lateral

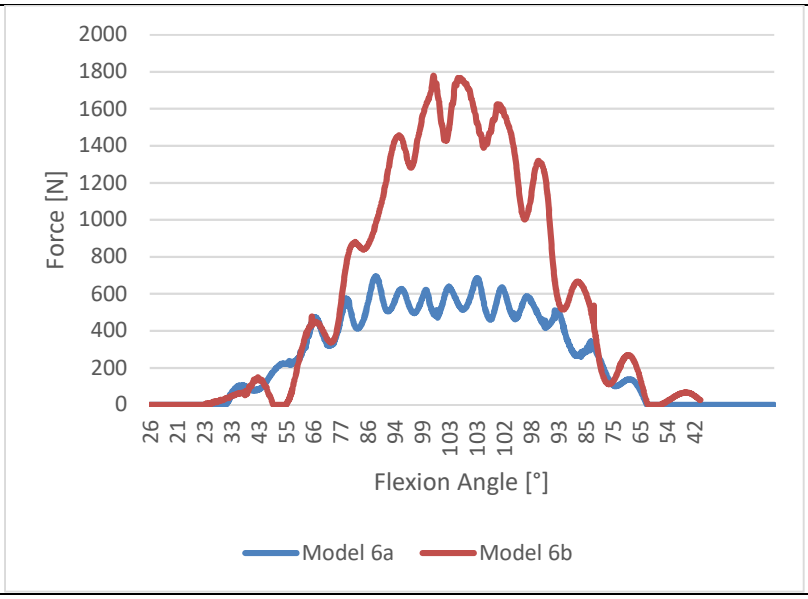

Figure 5.14 - Post-Cam Contact Forces

5.7 Seventh Model – MPFL and Lateral Retinaculum

The latest changes have brought the model to be more consistent with the real system: in fact in this last version trends and relations between the different contact forces result to be closer to the ones found in literature, as far as angular spans of action and values range are concerned [see Figure 89].

Furthermore, in this simulation the force component exerted by the three branches of the quadriceps [see Figure 88] and the axial component of the tibial constraint force [see Figure 87] were analyzed in more detail: these values in fact act as boundary conditions in the actual experimental tests, and therefore can be useful to be related to the other values obtained through the simulation.

As can be inferred from the graphs, the axial force exerted on the distal constraint tends to be constant as expected, while the muscular force adapts to the displacement of the femoral head following a sinusoidal trend.

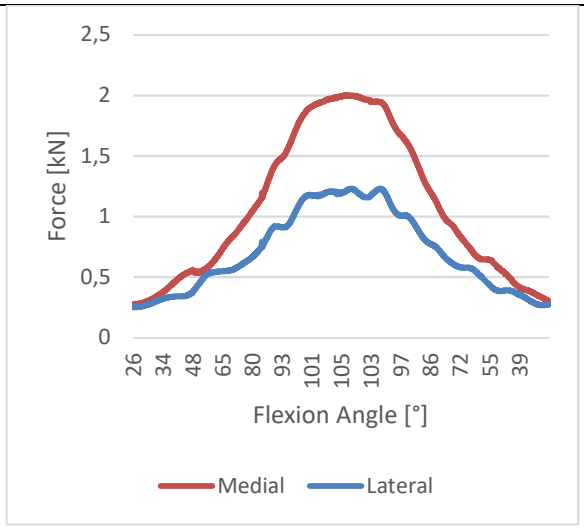

Figure 5.15 – Tibio-Femoral Contact Forces, Medial and Lateral Comparison

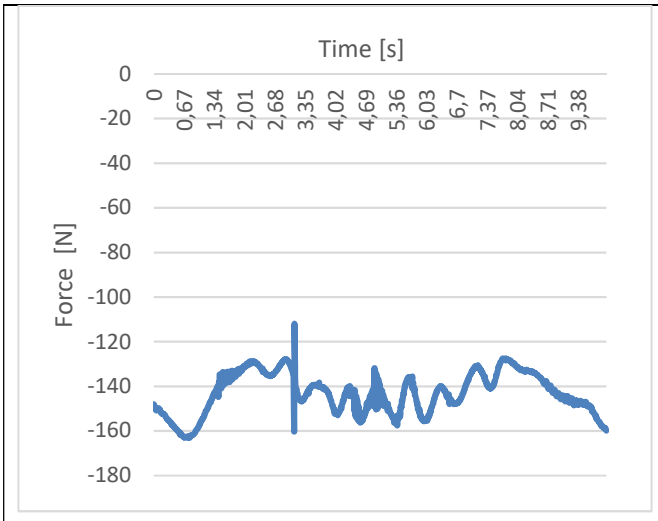

Figure 5.16 – Ankle Constraint Axial Force

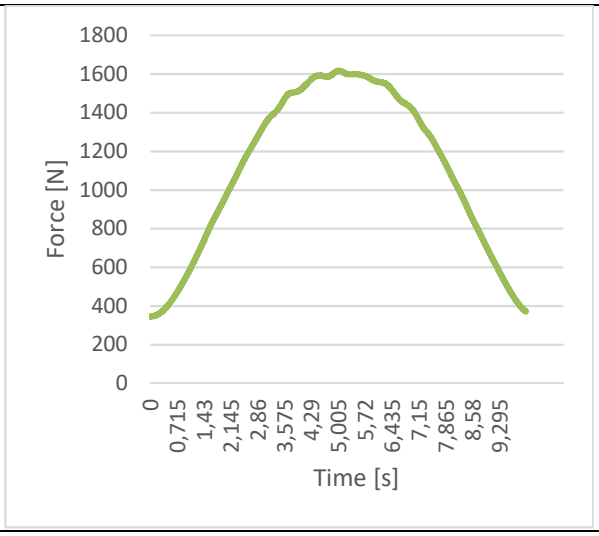

Figure 5.17 – Quadriceps Force

6. Validation and Future Developments

The results extrapolated from the last model were then used to perform a comparison with studies from the literature, taking however only the flexion related outputs into account.

6.1 Comparison

6.1.1 Kinematics

The results related to the intra-extra rotation angle during flexion [see Figure 92] are similar to the ones studied in literature[53] [see Figure 93] for a squat execution in presence of quadriceps but in total lack of hamstring. The range of values is matching and the trend follows the one experimentally obtained so, despite the presence of slight oscillations due to the not yet complete stability of the model, the result can be considered acceptable.

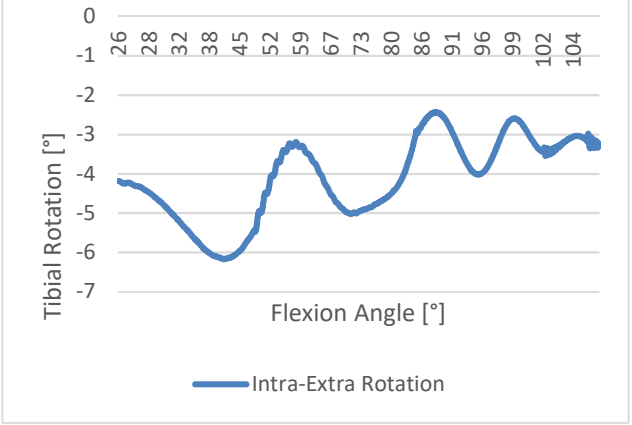

Figure 6.1 – Intra-Extra Rotation from SimPack Model

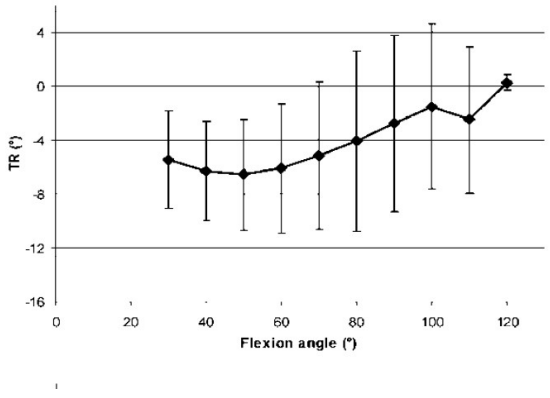

Figure 6.2 – Intra-Extra Rotation from experimental tests[53]

Concerning the anteroposterior displacement, different studies (Hill[54], Johal[55], Most[56], Victor[53]) have been reported in Figure 95 and 96 regarding the position of the two epicondylar centers; considering their midpoint as the center of the epicondylar axis (which is the analyzed in the numerical model developed [see Figure 94]), results show comparable trends and values.

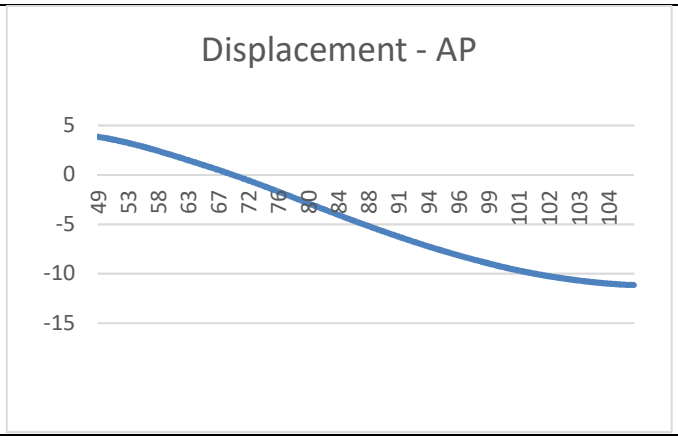

Figure 6.3 – Antero Posterior Displacement from SimPack Model

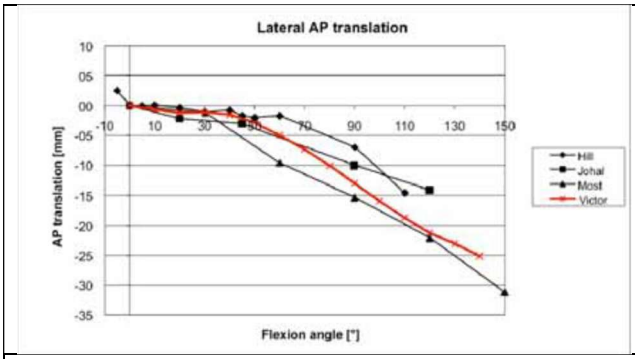

Figure 6.4 - Antero Posterior Displacement, Lateral Epicondyle[53]

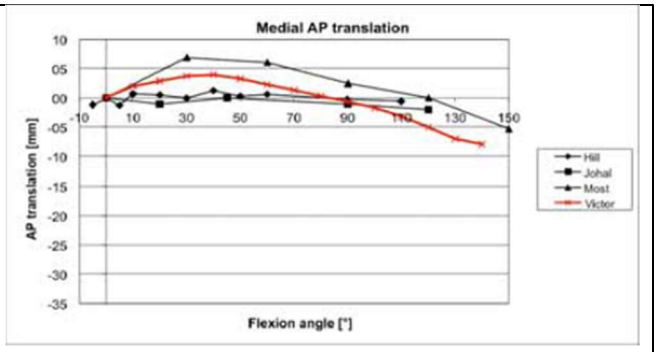

Figure 6.5 - Antero Posterior Displacement, Medial Epicondyle[53]

6.1.2 Kinetics

Comparing the tibiofemoral mediolateral contact forces [see Figure 97 99] with the ones obtained in literature [see Figure 98 100][57] (and here expressed relatively to an ideal body weight of 712 N), the trends appear to be similar. Despite the different conditions imposed lead the magnitudes obtained not to coincide with the one in literature, the ratio between the peak of the medial and lateral force obtained [see Figure 101] turns out to be comparable with the study [see Figure 102][57] thus making clear that the results are consistent with each other and therefore acceptable.

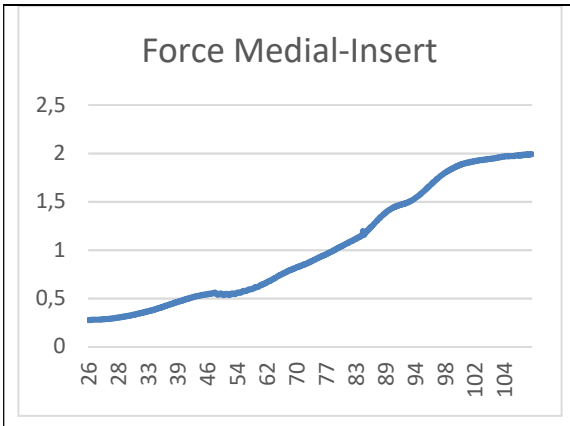

Figure 6.6 - Tibio-Femoral Contact Forces from SimPack Model, Medial

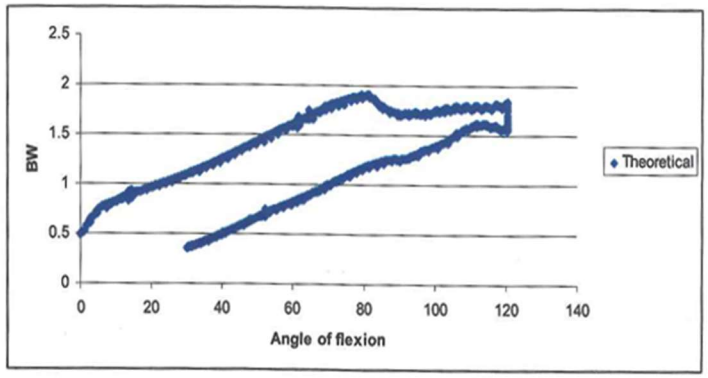

Figure 6.7 - Tibio-Femoral Contact Forces from Literature[57], Medial

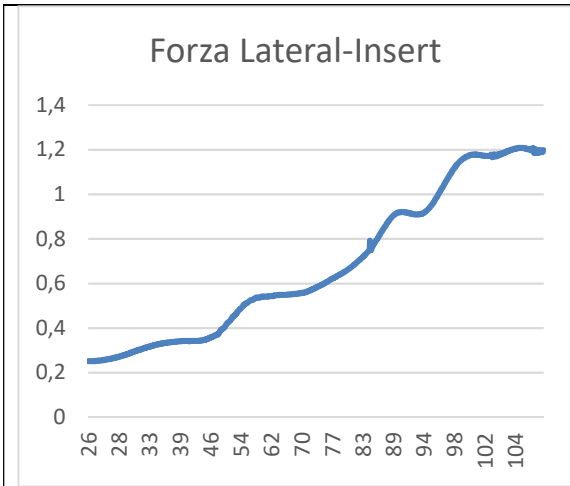

Figure 6.8 - Tibio-Femoral Contact Forces from SimPack Model, Lateral

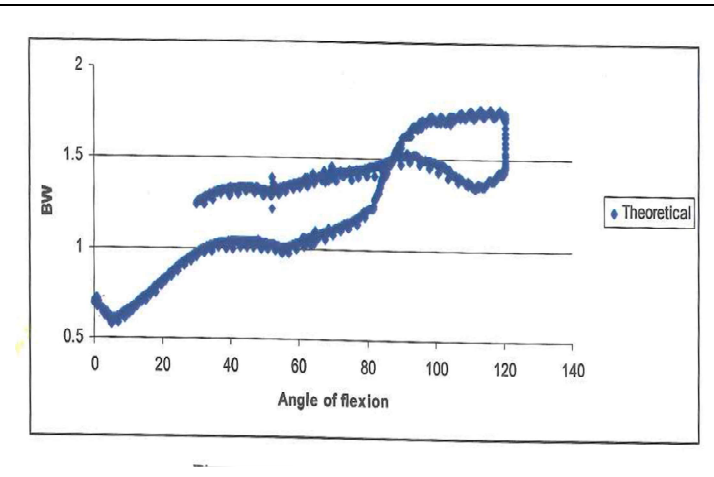

Figure 6.9 - Tibio-Femoral Contact Forces from Literature[57], Lateral

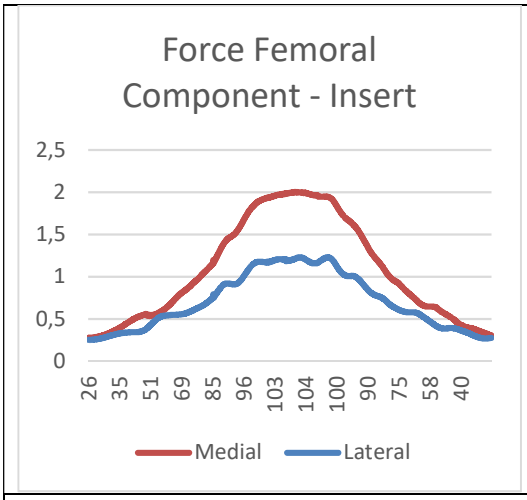

Figure 6.10 - Tibio-Femoral Contact Forces from SimPack Model, Medial and Lateral

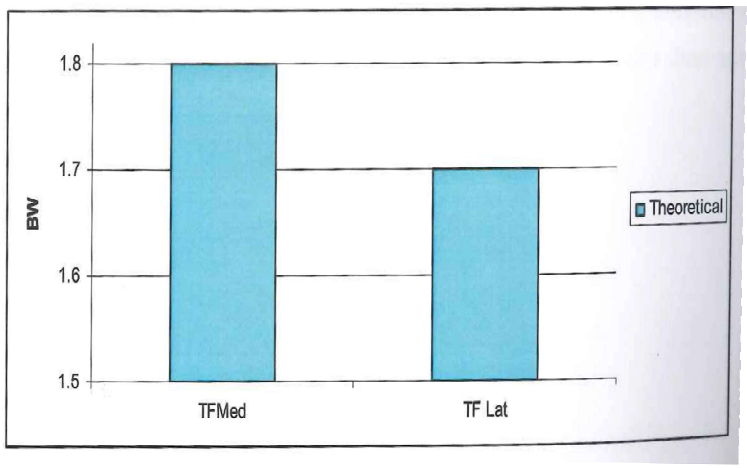

Figure 6.11 - Tibio-Femoral Contact Forces from Literature[57], Maximum Values Comparison

Similar situation can be found in patellofemoral sector, in which both the Model [see Figure 103] and the Literature study [see Figure 104][57] show an increasing trend up to about 60 ° of flexion and then a plateau (neglecting the slight oscillations due to the instability of the model).

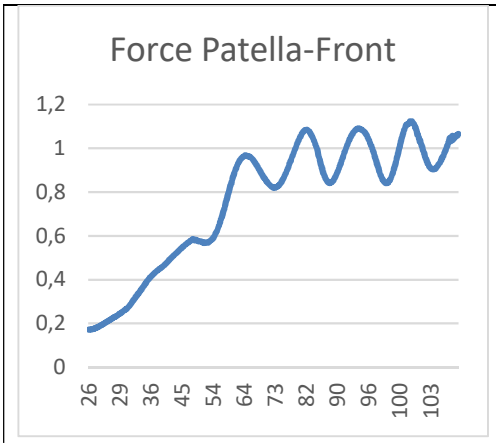

Figure 6.12 - Patello-Femoral Contact Forces from SimPack Model

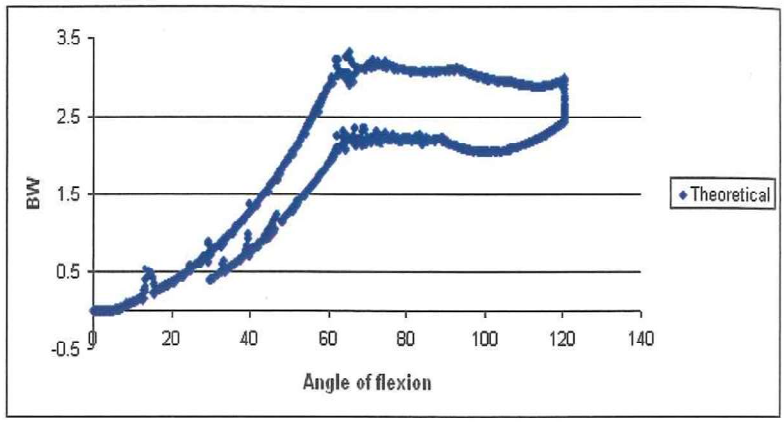

Figure 6.13 - Patello-Femoral Contact Forces from Literature[57]

Regarding the forces in the post-cam system, it is deductible how the outcomes follow a similar trend but with different magnitude. Another parameter taken in consideration was then the flexion angle corresponding to the contact between the two components: the graphs show similar angle for both the developed model [see Figure 105] and the literature [see Figure 106][57], and further confirmation can be obtained from the white paper[61] [see Figure 107]; this latter refers to the prosthesis model implemented in the simulator, and although the plotted parameter itself is not taken into consideration, it is evident how the contact takes place around 60 ° exactly like the model outputs.

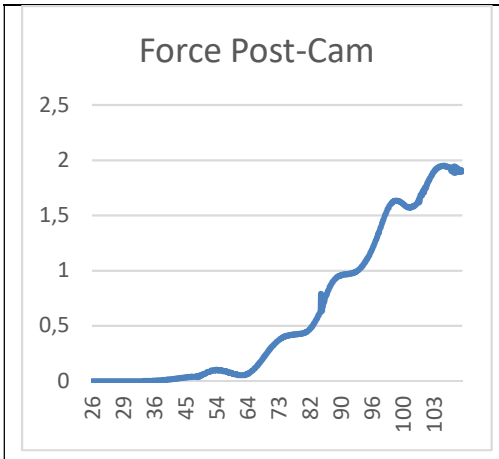

Figure 6.14 - Post-Cam Contact Forces from SimPack Model

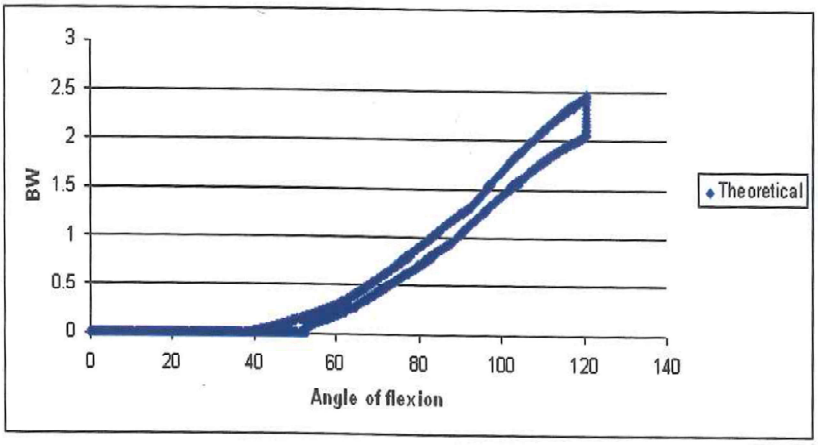

Figure 6.15 - Post-Cam Contact Forces from Literature[57]

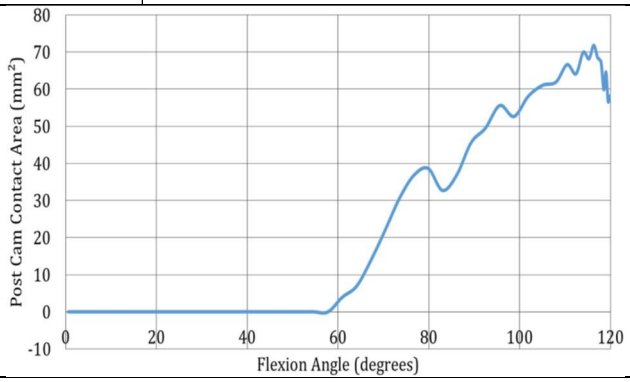

Figure 6.16 - Post-Cam Contact Area from Link Gemini white paper

The muscle activation pattern was compared with studies performed on a prosthetic knee with a BCR (bicruciate retaining)[53]; although this is a different prosthesis from the one implemented in the model developed, this comparison has been considered reliable since there is no significative difference in muscle action between the two situations when in the range of flexion angles analyzed[72].

Considering the offset of 400 N between the SimPack model [see Figure 108] and the experimental one [see Figure 109][53] (due to a different initial calibration), the range of values obtained also reflects those found experimentally in literature.

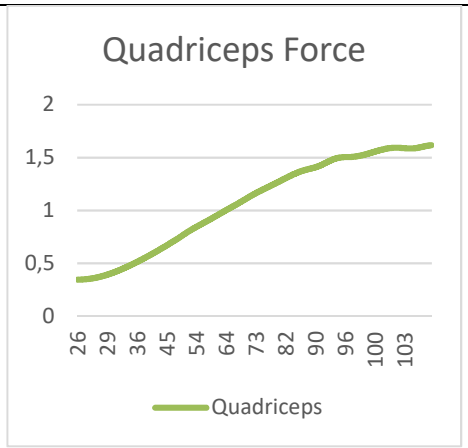

Figure 6.17 – Quadriceps Force from SimPack Model

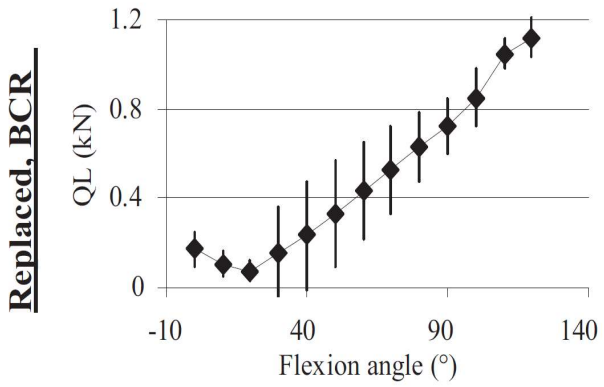

Figure 6.18 – Quadriceps Force from Experimental Test[53]

6.2 Future Developments

As previously analyzed, the outputs generated through this typology of simulation showed promising agreement with the experimental studies and data obtained with FEA; this result is a good incentive because, together with the relatively low computing time needed for this kind of simulations, it shows the potentiality of the MultiBody analysis in kinematic and kinetic studies applied to biomechanics.

The model obtained can therefore be considered a starting point for subsequent studies: dimensions and positioning of the prosthetic components or the tissues mechanical properties can be considered variable parameters to study the consequences of their changes on kinematics and kinetics; these data can then be used to predict the behavior of the replaced joint and thus help the surgeon in decision-making process. The possibility of using bone geometries extrapolated from TACs then allows the process to be patient specific and therefore more flexible, always maintaining computing times in a reasonable range.

7. Index of Figures

Chapter 1, Introduction - Native and Replaced Human Knee Joint

Chapter 2, Literature Research and State of the Art

8. Index of Tables

9. References

1) Miranda H et al., A prospective study on knee pain and its risk factors, Osteoarthritis Cartilage. 2002 Aug;10(8):623-30.

2) Blalock D. et al., Joint Instability and Osteoarthritis, Clin Med Insights Arthritis Musculoskelet Disord. 2015; 8: 15–23.

3) Alice J. Sophia Fox et al., The Basic Science of Articular Cartilage Structure, Composition, and Function, Sports Health. 2009 Nov; 1(6): 461–468.

4) Silverwood V. et al., Current evidence on risk factors for knee osteoarthritis in older adults: a systematic review and meta-analysis, Osteoarthritis Cartilage. 2015 Apr;23(4):507-15. doi: 10.1016/j.joca.2014.11.019. Epub 2014 Nov 29.

5) Behzad Heidari, Knee osteoarthritis prevalence, risk factors, pathogenesis and features: Part I, Caspian J Intern Med. 2011 Spring; 2(2): 205–212.

6) Saad M. Bindawas, Knee pain and health-related quality of life among older patients with different knee osteoarthritis severity in Saudi Arabia

7) Dinesh Bhatia et al., Current interventions in the management of knee osteoarthritis, J Pharm Bioallied Sci. 2013 Jan-Mar; 5(1): 30–38.

8) Paul W. Manner, Knee Replacement Implants, OrthoInfo AAOS

9) Hiroomi TATEISHI, Indications for Total Knee Arthroplasty and Choice of Prosthesis, JMAJ 44(4): 153–158, 2001

10) Sharkey PF et al., Factors influencing choice of implants in total hip arthroplasty and total knee arthroplasty: perspectives of surgeons and patients, J Arthroplasty. 1999 Apr;14(3):281-7.

11) Vertullo, Christopher & Grimbeek, Peter & Graves, Stephen & Lewis, Peter. (2017). Surgeon's Preference in Total Knee Replacement: A Quantitative Examination of Attributes, Reasons for Alteration and Barriers to Change. The Journal of Arthroplasty. 32. 10.1016/j.arth.2017.04.035.

12) Kyung Tae Kim et al., Causes of Failure after Total Knee Arthroplasty in Osteoarthritis Patients 55 Years of Age or Younger, Knee Surg Relat Res. 2014 Mar; 26(1): 13–19

13) Stephen Preston et al., Towards an understanding of the painful total knee: what is the role of patient biology?, Curr Rev Musculoskelet Med. 2016 Dec; 9(4): 388–395.

14) Abdulemir Ali et al., Dissatisfied patients after total knee arthroplasty -A registry study involving 114 patients with 8–13 years of follow-up, Acta Orthop. 2014 Jun; 85(3): 229–233.

15) Christen B. (2015) 11 Material Failure of Total Knee Replacement. In: Hirschmann M., Becker R. (eds) The Unhappy Total Knee Replacement. Springer, Cham

16) Kei Osano et al., The Effect of Malrotation of Tibial Component of Total Knee Arthroplasty on Tibial Insert during High Flexion Using a Finite Element Analysis, ScientificWorldJournal. 2014; 2014: 695028.

17) Matsumoto T., Kuroda R. (2015) 14 Malposition and Malorientation After Total Knee Replacement. In: Hirschmann M., Becker R. (eds) The Unhappy Total Knee Replacement. Springer, Cham

18) S.A.W.van de Groes et al., Effect of medial–lateral malpositioning of the femoral component in total knee arthroplasty on anterior knee pain at greater than 8 years of follow-up., The Knee Volume 21, Issue 6, December 2014, Pages 1258-1262

19) Kang et al., Malpositioning of Prosthesis: Patient-specific Total Knee Arthroplasty Versus Standard Off-the-Shelf Total Knee Arthroplasty, JAAOS Global Research & Reviews: July 2017 - Volume 1 - Issue 4 - p e020

20) Knee Implants Market Analysis By Procedure Type (Total, Partial, Revision Knee Replacement), By Component Type (Fixed-Bearing, Mobile-Bearing Implants), And Segment Forecasts To 2024

21) Kurtz et al. J Bone Joint Surg Am 2007;89:780-785

22) CDC/NCHS, National Hospital Discharge Survey, 2000-2010

23) Grood ES, Suntay WJ., A joint coordinate system for the clinical description of three-dimensional motions: application to the knee, J Biomech Eng. 1983 May;105(2):136-44.

24) Xavier Gasparutto et al., Kinematics of the Normal Knee during Dynamic Activities: A Synthesis of Data from Intracortical Pins and Biplane Imaging, Applied Bionics and BiomechanicsVolume 2017, Article ID 1908618, 9 pages

25) Deepak Kumar et al., Knee Joint Loading during Gait in Healthy Controls and Individuals with Knee Osteoarthritis, Osteoarthritis Cartilage. 2013 Feb; 21(2): 298–305.

26) Trepczynski A et al., Patellofemoral joint contact forces during activities with high knee flexion, J Orthop Res. 2012 Mar;30(3):408-15.

27) Tiré, Jan & Victor, Jan & de baets, Patrick & Verstraete, Matthias. (2015). Control of the boundary conditions of a dynamic knee simulator. International Journal Sustainable Construction & Design. 6. 10.21825/scad.v6i2.1125.

28) Maletsky, Lorin & M Hillberry, Ben. (2005). Simulating Dynamic Activities Using a Five-Axis Knee Simulator. Journal of biomechanical engineering. 127. 123-33. 10.1115/1.1846070.

29) http://www.lifemodeler.com/products/kneesim/

30) http://www.lifemodeler.com/products/lifemod/

31) Amber N. Reeve et al., Verification of a Dynamic Knee Simulator Computational Model, ASME 2008 Summer Bioengineering Conference

32) http://www.simpack.com/

33) https://www.solidworks.com/

34) https://www.3ds.com/products-services/simulia/products/abaqus/

35) Hippmann, G.: An Algorithm for Compliant Contact Between Complexly Shaped Surfaces in Multibody Dynamics. Proc. of the IDMEC/IST, Lisbon, Portugal (2003)

36) Johnson, K.L.: Contact Mechanics, Cambridge University Press UK (1987)].

37) SimPack Documentation

38) https://www.linkorthopaedics.com/en/for-the_physician/products/knie/primary/gemini-sl-total-knee-replacement

39) Bert Parcells, TKA BONE CUTS, https://hipandkneebook.com/tja-publication-blog/2017/3/14/tka-bone-cuts

40) Innocenti, B., Fekete, G., Pianigiani, S. 2018. Biomechanical Analysis of Augments in Revision Total Knee Arthroplasty. J. Biomech Eng 140(11), 111006 (10 pages). [IF=1.916]

41) Zair F et al., Changes in human knee ligament stiffness secondary to osteoarthritis, Journal of Orthopaedic Research 20 (2002) 204-207

42) Akira Saito et al., Anatomical cross-sectional area of the quadriceps femoris and sit-to-stand test score in middle-aged and elderly population: development of a predictive equation, J Physiol Anthropol. 2017; 36: 3.

43) Innocenti B et al., How accurate and reproducible are the identification of cruciate and collateral ligament insertions using MRI?, Knee. 2016 Aug;23(4):575-81

44) https://www.physio-pedia.com/Medial_Collateral_Ligament_of_the_Knee

45) LaPrade, Robert & Dean, Chase & Chahla, Jorge & Schon, Jason. (2017). Fibular Collateral Ligament and the Posterolateral Corner.

47) Pierre Andonian et al., Shear-Wave Elastography Assessments of Quadriceps Stiffness Changes prior to, during and after Prolonged Exercise: A Longitudinal Study during an Extreme Mountain Ultra-Marathon, PLoS One. 2016; 11(8): e0161855.

48) http://animatlab.com/Help/Documentation/Biomechanical-Editor/Biomechanical-Body-Parts/Linear-Hill-Muscle

49) Stäubli HU et al., Mechanical tensile properties of the quadriceps tendon and patellar ligament in young adults, Am J Sports Med. 1999 Jan-Feb;27(1):27-34.

50) https://simtk.org/

51) Mirco Herbort et al., Bio-mechanical Properties of a New MPFL Reconstruction Technique Using Quadriceps Tendon in Comparison to the Intact MPFL. A Human Cadaveric Study, Arthroscopy , Volume 29 , Issue 10 , e84 - e85

52) Azhar M. Merican et al., The structural properties of the lateral retinaculum and capsular complex of the knee, J Biomech. 2009 Oct 16; 42(14): 2323–2329

53) Jan Victor, A comparative study on the biomechanics of the native human knee joint and total knee arthroplasty

54) Hill et al., Tibiofemoral movement 2: the loaded and unloaded living knee studied by MRI, J Bone Joint Surg Br 82-B: 1196-1198

55) Johal, P, Williams, A, Wragg, P, et al. 2005. Tibio-femoral movement in the living knee. A study of weight bearing and non-weight bearing knee kinematics using `interventional' MRI. Journal of Biomechanics 38: 269-276.

56) Most, E, Axe, J, Rubash, H, Li, G. 2004. Sensitivity of the knee joint kinematics calculation to selection of flexion axes. Journal of Biomechanics 37: 1743-1748.

57) Silvia Pianigiani, Numerical sensitivity analysis in several TKA designs during squatting

58) Physiopedia contributors, 'Total knee arthroplasty', *Physiopedia, ,* 18 July 2018, 06:47 UTC

59) Mark A.Baldwin et al., Dynamic finite element knee simulation for evaluation of knee replacement mechanics, Journal of Biomechanics Volume 45, Issue 3, 2 February 2012, Pages 474-483

60) Hirschmann, M.T. & Müller, W. Knee Surg Sports Traumatol Arthrosc (2015) 23: 2780. https://doi.org/10.1007/s00167-015-3619-3

61) Bernardo Innocenti, GEMINI® SL® Fixed Bearing PS: Biomechanical Analysis of the Post-Cam System

62) Bernardo Innocenti, Contact forces in several TKA designs during squatting: A numerical sensitivity analysis, Journal of Biomechanics 44 (2011) 1573–1581

63) Silvia Pianigiani, Tibio-femoral kinematics in different total knee arthroplasty designs during a loaded squat: A numerical sensitivity study, Journal of Biomechanics 45 (2012) 2315–2323

64) Eckhoff D. G., Functional Anatomy of the knee, Total Knee arthroplasty, 2005

65) Fick R., Mechanil des Kniegelenkes. In: von Bardeleben (ed) Handuch der Anatomie des Menshen, Band 2, 1, vol 3. Gustav Fisher, Jena, 1911

66) Weber W., Weber F., Mechanism of the human walking apparatus. Sect 4: The Knee. Springer-Verlag, Berlin Heindelberg New York, 1992

67) Martini, Timmons, Tallish, Anatomia umana

68) C. Abbriciani et al., Biomeccanica dell'articolazione del ginocchio, Biomeccanica ortopedica e traumatica

69) Kettelkamp D., An electromagnetic study of the knee in normal gait, J Bone Joint Surgery, 52A:775-790, 1970

70) Alice J. S. Fox et al., The Basic Science of Human Knee Menisci, Sports Health. 2012 Jul; 4(4): 340–351.

71) Diana Bitar and Javad Parvizi, Biological response to prosthetic debris, World J Orthop. 2015 Mar 18; 6(2): 172–189.

72) Osmani, Feroz A et al. “The utility of bicruciate-retaining total knee arthroplasty” Arthroplasty today vol. 3,1 61-66. 27 Dec. 2016, doi:10.1016/j.artd.2016.11.004